BBA - Molecular Basis of Disease 1865 (2019) 1627–1641

Contents lists available at ScienceDirect

BBA - Molecular Basis of Disease

journal homepage: www.elsevier.com/locate/bbadis

Mitochondrial ALDH2 protects against lipopolysaccharide-induced myocardial contractile dysfunction by suppression of ER stress and autophagy

Jiaojiao Pang[a,b,1], Hu Peng[c,1], Shuyi Wang[a,1], Xihui Xu[a], Feng Xu[b], Qiurong Wang[a], Yuanzhuo Chen[c], Linzi A. Barton[a], Yuguo Chen[b,*], Yingmei Zhang[a,d,*], Jun Ren[a,d,*]

[a] Center for Cardiovascular Research and Alternative Medicine, University of Wyoming College of Health Sciences, Laramie, WY 82071, USA
[b] Department of Emergency Medicine and Chest Pain Center, Qilu Hospital of Shandong University, Jinan, Shandong 250012, China
[c] Department of Emergency, Shanghai Tenth People's Hospital, School of Medicine Tongji University, Shanghai 200072, China
[d] Department of Cardiology, Shanghai Institute of Cardiovascular Diseases, Fudan University Zhongshan Hospital, Shanghai 200032, China

ARTICLE INFO

Keywords:
Lipopolysaccharide
Cardiac
ER stress
Autophagy
ALDH2
Endosome

ABSTRACT

Lipopolysaccharide (LPS), an essential component of outer membrane of the Gram-negative bacteria, plays a pivotal role in myocardial anomalies in sepsis. Recent evidence depicted an essential role for mitochondrial aldehyde dehydrogenase (ALDH2) in cardiac homeostasis. This study examined the effect of ALDH2 on endotoxemia-induced cardiac anomalies. Echocardiographic, cardiac contractile and intracellular Ca^{2+} properties were examined. Our results indicated that LPS impaired cardiac contractile function (reduced fractional shortening, LV end systolic diameter, peak shortening, maximal velocity of shortening/relengthening, prolonged relengthening duration, oxidation of SERCA, and intracellular Ca^{2+} mishandling), associated with ER stress, inflammation, O_2^- production, increased autophagy, CAMKKβ, phosphorylated AMPK and suppressed phosphorylation of mTOR, the effects of which were significantly attenuated or negated by ALDH2. LPS promoted early endosomal formation (as evidenced by RAB4 and RAB5a), apoptosis and necrosis (MTT and LDH) while decreasing late endosomal formation (RAB7 and RAB 9), the effects were reversed by ALDH2. *In vitro* study revealed that LPS-induced SERCA oxidation, autophagy and cardiac dysfunction were abrogated by ALDH2 activator Alda-1, the ER chaperone TUDCA, the autophagy inhibitor 3-MA, or the AMPK inhibitor Compound C. The beneficial effect of Alda-1 against LPS was nullified by AMPK activator AICAR or rapamycin. CAMKKβ inhibition failed to rescue LPS-induced ER stress. Tunicamycin–induced cardiomyocyte dysfunction was ameliorated by Alda-1 and autophagy inhibition, the effect of which was abolished by rapamycin. These data suggested that ALDH2 protected against LPS-induced cardiac anomalies *via* suppression of ER stress, autophagy in a CAMKKβ/AMPK/mTOR-dependent manner.

1. Introduction

Sepsis, clinically presented as the systemic inflammatory response syndrome (SIRS), is a critical health issue with a high mortality of 15%–20% [1,2]. Septic cardiomyopathy, one of the most devastating multi-organ dysfunctions in septic shock, is accompanied with an overtly increased mortality rate of ~70%–90% [2–4]. Survivors of septic cardiomyopathy often suffer from long-term complications and poor cardiovascular health. Although much progress has been archived for the pathogenesis and clinical management of sepsis [2,5], targeted therapy for septic cardiomyopathy is still lacking due to an incomplete understanding for the precise mechanism behind the pathogenesis of this comorbidity. Recent evidence suggested a pivotal role for interrupted redox and endoplasmic reticulum (ER) homeostasis in the onset of septic injury [6,7]. ER stress is an intracellular membranous network governing intracellular Ca^{2+} storage, folding, processing of proteins, lipid and sterol [8]. Disturbed ER homeostasis by pathological stimuli such as endotoxin may result in a state of ER stress and pathological unfolded protein response (UPR) [9,10], leading to various forms of cell death including necrosis, apoptosis, necroptosis and autophagic death

* Corresponding authors at: Center for Cardiovascular Research and Alternative Medicine, University of Wyoming College of Health Sciences, Laramie, WY 82071, USA and Qilu Hospital of Shandong University, Jinan, Shandong 250012, China.
E-mail addresses: chen919085@126.com (Y. Chen), zhangym197951@126.com (Y. Zhang), jren@uwyo.edu (J. Ren).
[1] Equal contribution.

https://doi.org/10.1016/j.bbadis.2019.03.015
Received 8 December 2018; Received in revised form 13 March 2019; Accepted 28 March 2019
Available online 01 April 2019

(autosis) [11,12]. More recent evidence from our group and others has also suggested a pivotal role for autophagy in the pathogenesis of septic cardiomyopathy [13–15]. Although our earlier reports suggested a unique beneficial effect of antioxidants (such as metallothionein and catalase) and ER chaperone in septic cardiomyopathy [16,17], antioxidant treatment failed to effectively rescue altered autophagy and inflammation in septic hearts [16], thus raising the issue of interplay among ER stress, oxidative stress and autophagy in septic cardiomyopathy.

Mitochondrial aldehyde dehydrogenase (ALDH2) is an essential enzyme to detoxify reactive aldehydes [18]. Genetic polymorphism of *ALDH2* exists in humans with the mutant *ALDH2*2* allele, severely compromising its enzymatic activity [18]. Prevalence of *ALDH2*2* is nearly 40% in Asian population [19]. Recent evidence has suggested an important role for ALDH2 in cardiometabolic diseases including ischemia and reperfusion injury, heart failure, alcoholic cardiomyopathy and diabetes [20–26]. However, the role of ALDH2 in sepsis remains largely unknown. Given the eminent role for ALDH2 gene in cardiovascular function [20–26], this study examined the impact of ALDH2 on cardiac function in endotoxemia. Since ER, autophagy, oxidative stress and inflammation have been indicated to mediate ALDH2-associated cardiovascular responses [20,27–30], levels of ER stress, autophagy, O_2^- production and proinflammatory markers were monitored in WT and ALDH2 transgenic mice challenged with lipopolysaccharides (LPS). Levels of key autophagy regulatory molecules including AMP-dependent protein kinase (AMPK), mTOR and Ca^{2+}/calmodulin-dependent protein kinase kinase-β (CaMKKβ), an upstream signal for AMPK [31], and a downstream effector for UPR [32,33] were also evaluated in murine hearts. Given the important role of recycling endosomes (involving the budding and fusion events of membrane trafficking) in the recruitment of autophagy proteins and endocytosis [34], protein markers of early (RAB4 and RAB5a) and late (RAB7 and RAB 9) endosome formation [35] were monitored along with cell death markers. These Ras-related small GTPases of the Rab family are localized in part or mainly to the ER to regulate ER tabulation, ER contacts with other organelles, membrane trafficking among Golgi complex, endosome, and autophagosome formation [35]. To discern the connection between cell stress and intracellular Ca^{2+} homeostasis, oxidation of sarco(endo)plasmic reticulum-Ca^{2+}-ATPase (SERCA) was monitored.

2. Methods and materials

2.1. Experimental animals, LPS treatment and measurement of ALDH2 activity

All animal experimental procedures performed were approved by the Animal Care and Use Committees at the University of Wyoming (Laramie, WY) and Fudan University Zhongshan Hospital (Shanghai, China). All procedures were in accordance with the NIH Guide for the Care and Use of Laboratory Animals. Production of ALDH2 transgenic mice was described previously [26]. In brief, 4–5 month-old male mice were housed in a climate-controlled environment (22.8 ± 2.0 °C, 45–50% humidity) with a 12/12–light/ dark cycle with access to food and water *ad libitum* until experimentation. On the day of experimentation, ALDH2 and WT mice were injected intraperitoneally with 4 mg/kg *Escherichia coli* O55:B5 LPS dissolved in sterile saline or an equivalent volume of pathogen-free saline for control. Six hours later, mice were sacrificed [36]. ALDH2 activity was measured in 33 mM sodium pyrophosphate containing 0.8 mM NAD^+, 15 μM propionaldehyde and 0.1 ml protein extract. Propionaldehyde, the substrate of ALDH2, was oxidized in propionic acid, while NAD^+ was reduced to NADH to estimate ALDH2 activity. NADH was determined by spectrophotometric absorbance at 340 nm. ALDH2 activity was expressed as nmol NADH/min/mg protein [37].

2.2. Isolation of cardiomyocytes and in vitro drug treatment

After ketamine sedation, hearts were rapidly removed and mounted onto a temperature-controlled (37 °C) Langendorff system. The hearts were digested for 10–15 min with a modified Tyrode solution containing Liberase Blendzyme 4 (Hoffmann-La Roche Inc., Indianapolis, IN). The modified Tyrode solution (pH 7.4) contained the following (in mM): NaCl 135, KCl 4.0, $MgCl_2$ 1.0, HEPES 10, NaH_2PO_4 0.33, glucose 10, and butanedione monoxime 10, and the solution was gassed with 5% CO_2-95% O_2. Tissue pieces were gently agitated and pellet of cells was resuspended. Extracellular Ca^{2+} was added incrementally back to 1.20 mM over a period of 30 min. Only rod-shaped cardiomyocytes with clear sarcomere striations were selected for mechanical studies [27]. Cardiomyocyte yield was approximately 65–75% which was not affected by LPS challenge. To assess the role of ALDH2, ER stress, CAMKKβ, AMPK and autophagy in LPS-induced cardiomyocyte dysfunction and cell survival, cardiomyocytes from WT mice were exposed to LPS (4 μg/ml) [16] for 4 h in the presence or absence of the ALDH2 inducer Alda-1 (20 μM) [21], the ER chaperone tauroursodeoxycholic acid (TUDCA, 500 μM) [38], the CAMKKβ inhibitor STO-609 (5 μg/ml) [39], the AMPK inhibitor Compound C (10 μM) [40], the AMPK inducer AICAR (500 μM) [41], the mTOR inhibitor rapamycin (5 μM) [42] or the autophagy inhibitor 3-methyladenine (3-MA, 10 mM) [43] prior to biochemical or mechanical assessment. To assess the role of ER stress, cardiomyocytes from WT mice were exposed to tunicamycin (3 μg/ml) [44] for 4 h in the presence or absence of 3-MA (10 mM) or Alda-1 (20 μM) with or without rapamycin (5 μM) prior to mechanical assessment.

2.3. Electron microscopy

The ultrastructure of cardiomyocytes was evaluated using transmission electron microscopy. In brief, mouse heart from each experiment group was perfused and fixed with PIPES-buffered formaldehyde-glutaraldehyde. Left ventricular myocardium was taken from the mid-ventricular region and was trimmed to 1-mm^3 blocks. The blocks were fixed using a 10:1 fluid/tissue ratio overnight at 4 °C. After washing with PIPES buffer along with 2% sucrose (pH 7.4), myocardial blocks were further processed in PIPES buffered 1% OsO_4 along with 2% sucrose and 1.5% $K_3FE(CN)_6{\cdot}3H_2O$ overnight at 22–24 °C. The blocks were then dehydrated using graded ethanol and propylene oxide, and were ultimately enclosed in Epon/Araldite. RMC-MTXL ultramicrotome and a Diatome diamond knife were used to obtain thin sections. Sections were labeled with lead citrate and uranyl acetate (in absolute ethanol). Micrographic pictures were taken using a Hitachi 7500 transmission electron microscope [45].

2.4. Echocardiography

Cardiac geometry and function were evaluated in anesthetized (~1% isoflurane inhalation) mice using the 2-dimensional (2-D) guided M-mode echocardiography (Phillips Sonos 5500) equipped with a 15–6 MHz linear transducer. The heart was imaged in the 2-D mode in parasternal long-axis view with a depth setting of 2 cm. M mode cursor was positioned perpendicular to the interventricular septum and posterior wall of left ventricle (LV) at the level of papillary muscles from 2-D mode. LV anterior and posterior wall dimensions during diastole (LVPWd) and systole (LVPWs) were recorded from three consecutive cycles in M-mode using the method adopted by the American Society of Echocardiography. Fractional shortening was calculated from LV end-diastolic (LVEDD) and end-systolic (LVESD) diameters using the equation (LVEDD − LVESD) / LVEDD × 100. Heart rates were averaged from 10 cardiac cycles [36].

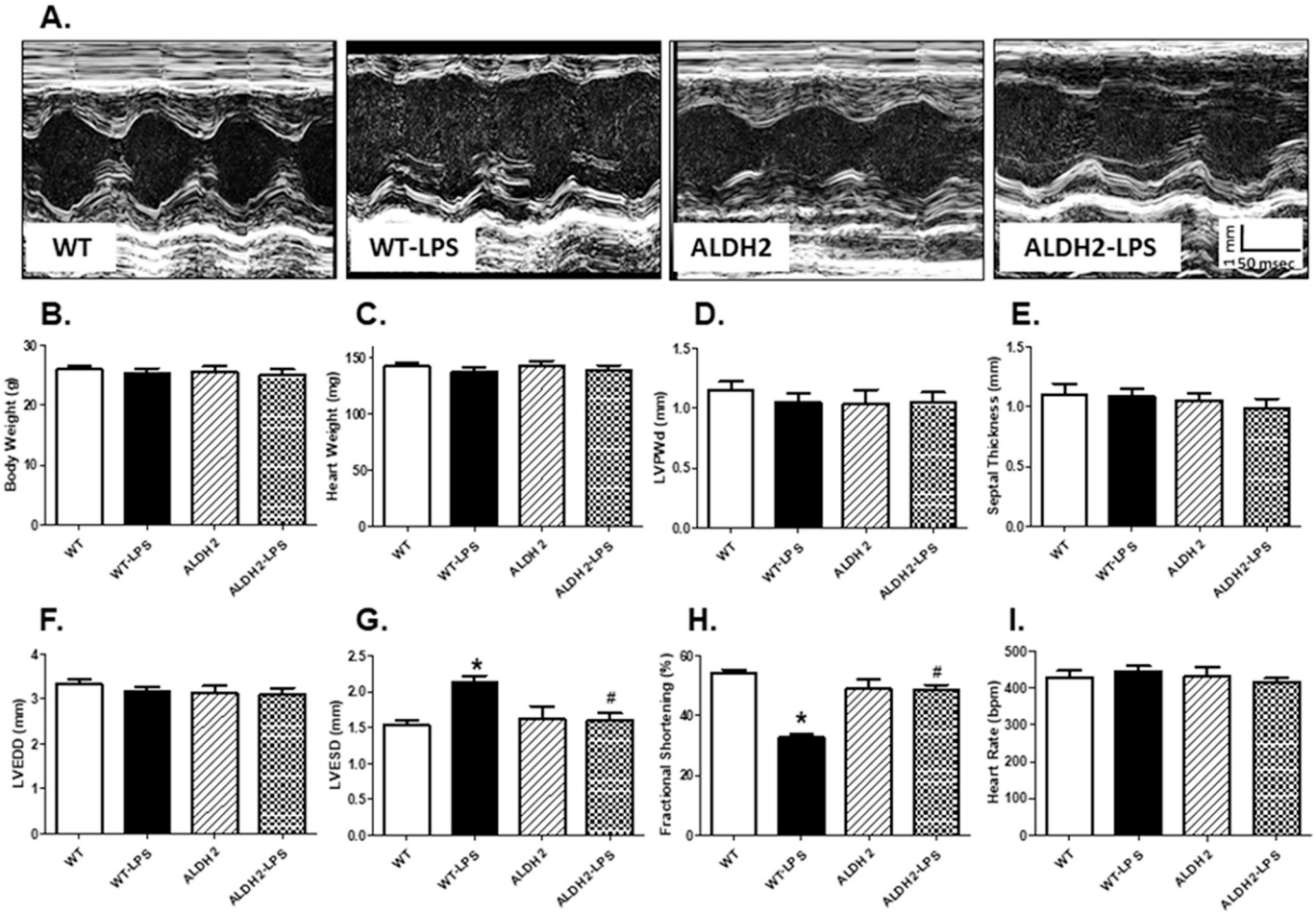

Fig. 1. Effect of ALDH2 overexpression on LPS-induced echocardiographic changes. WT and ALDH2 mice were challenged with LPS (4 mg/kg, i.p. for 6 h) prior to assessment of echocardiographic properties. A: Representative echocardiographic images from all 4 mouse groups; B: body weight; C: heart weight; D: LV posterior wall thickness in diastole (LVPWd); E: septal thickness; F: LV end diastolic diameter (LVEDD); G: LV end systolic diameter (LVESD); H: fractional shortening; and I: heart rate. Mean ± SEM; n = 8–9 mice/group, *p < 0.05 *vs.* WT group; #p < 0.05 *vs.* WT–LPS group.

2.5. Cell shortening/relengthening

Mechanical properties of cardiomyocytes were assessed using a SoftEdge Myocam (IonOptix, Milton, MA). Cardiomyocytes were placed in a chamber mounted on the stage of an inverted microscope (Olympus IX-70) and superfused (~2 ml/min at 25 °C) with a Krebs-Henseleit bicarbonate buffer containing 1 mM $CaCl_2$. Myocytes were field stimulated at 0.5 Hz. Cell shortening was assessed including peak shortening (PS), indicating peak contractility; time-to-PS (TPS), indicating contraction duration; time-to-90% relengthening (TR_{90}), indicating relaxation duration; and maximal velocities of shortening/relengthening (± dL/dt), indicating maximal pressure development and decline [27].

2.6. Intracellular Ca^{2+} transient

Cardiomyocytes were loaded with fura-2/AM (0.5 μM) for 10 min and fluorescence measurements were recorded with dual-excitation fluorescence photo multiplier tube (PMT, Ionoptix). Cardiomyocytes were placed on an Olympus IX-70 inverted microscope and imaged through a Fluor 40× oil objective. Cells were exposed to light emitted by a 75-W lamp and passed through 360 nm or a 380 nm filter, while being stimulated to contract at 0.5 Hz. Fluorescence emissions were detected between 480 nm and 520 nm by PMT after first illuminating cells at a 360 nm for 500 ms, then at 380 nm for the duration of the recording protocol (333 Hz sampling rate). The 360 nm excitation scan was repeated at the end of the protocol and qualitative changes in intracellular Ca^{2+} levels were inferred from the ratio of fura-2 fluorescence intensity at two wavelengths (360/380). Fluorescence decay time was assessed as an indication of intracellular Ca^{2+} clearing. Single exponential curve fit was applied to calculate intracellular Ca^{2+} decay rate [46].

2.7. Intracellular fluorescence measurement of superoxide (O_2^-)

Intracellular O_2^- was monitored by changes in fluorescence intensity from intracellular probe oxidation. In brief, cardiomyocytes were loaded with 5 μM dihydroethidium (DHE) (Molecular Probes, Eugene, OR) for 30 min at 37 °C. Cells were evaluated using an Olympus BX-51 microscope with Olympus MagnaFire™ SP digital camera. Fluorescence was calibrated using InSpeck microspheres (Molecular Probes) and was quantitated using an ImagePro analysis software (Media Cybernetics, Silver Spring, MD) [10].

2.8. Caspase-3 and lactate dehydrogenase (LDH) assay

Mouse blood samples were collected and serum prepared. Serum LDH levels were evaluated as an index for cardiac injury using an ELISA kit. Myocardial tissues were homogenized and centrifuged at 10,000 ×*g* at 4 °C for 10 min. Pellets were lysed in ice-cold lysis buffer (50 mM HEPES, 0.1% CHAPS, 1 mM dithiothreitol, 0.1 mM EDTA, 0.1% NP40). Following tissue lysis, 70 μl of reaction buffer was added before incubation with caspase-3 colorimetric substrate (Ac-DEVD-pNA, 20 μl)

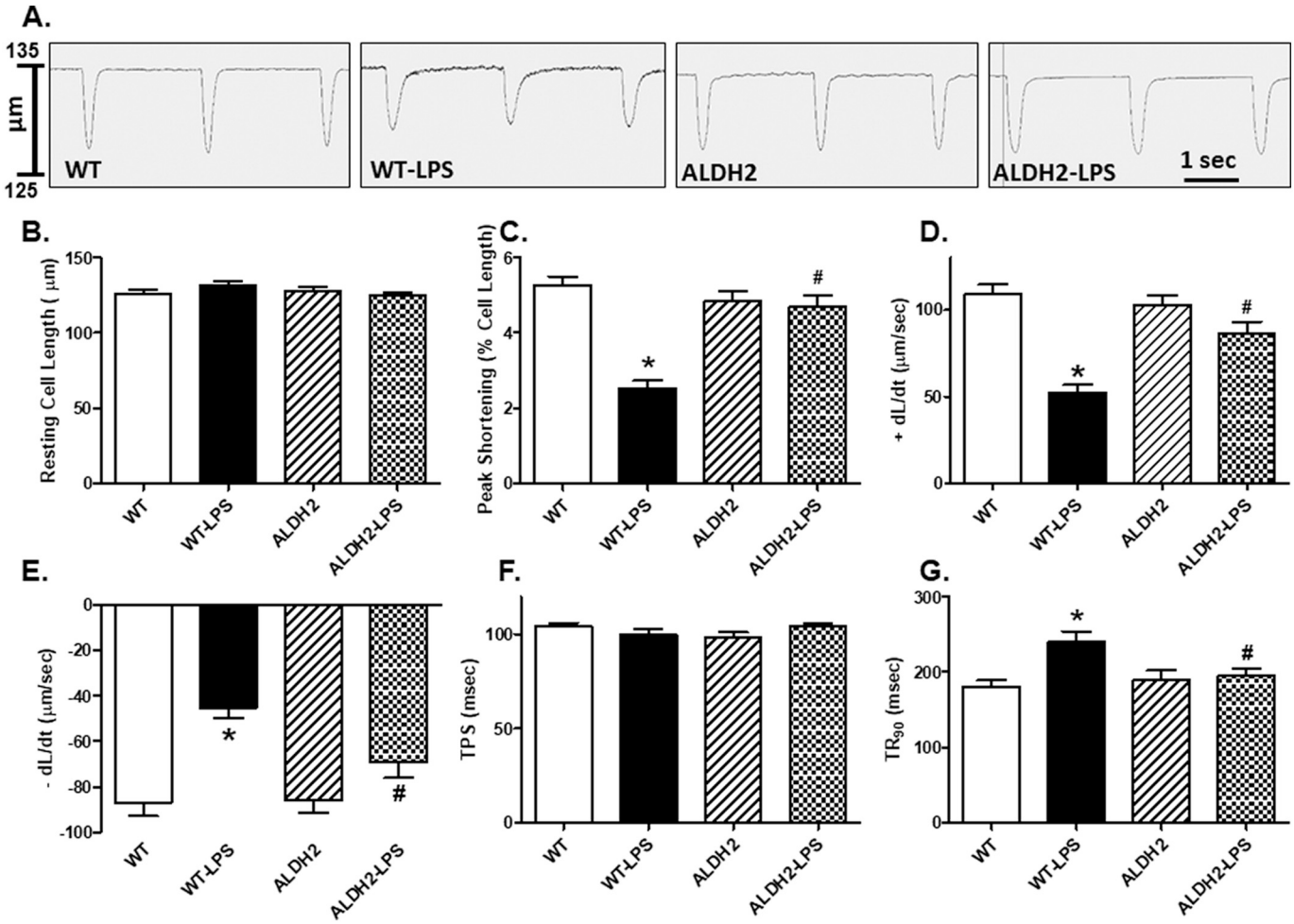

Fig. 2. Contractile properties of cardiomyocytes from WT and ALDH2 transgenic mice treated with or without LPS (4 mg/kg, i.p. for 6 h). A: Representative cell shortening traces from all 4 mouse groups; B: resting cell length; C: peak shortening (PS); D: maximal velocity of shortening (+dL/dt); E: maximal velocity of relengthening (−dL/dt); F: time-to-PS (TPS); and G: time-to-90% relengthening (TR_{90}). Mean ± SEM, n = 122 cells from 6 mice per group. *$p < 0.05$ *vs.* WT group, #$p < 0.05$ *vs.* WT-LPS group.

for 1 h (at 37 °C). Caspase in the sample was allowed to cleave the chromophore p-NA from its substrate. Samples were then read with a microplate reader at 405 nm. Caspase-3 activity was expressed as picomoles of pNA released per microgram of protein per minute [47].

2.9. MTT assay for cell viability

Fresh murine cardiomyocytes from various experimental groups were plated in microtiter plate at a density of 3×10^5 cells/ml prior to addition of MTT to with a final concentration of 0.5 mg/ml, and plates were incubated for 2 h at 37 °C. The formazan crystals were dissolved in dimethyl sulfoxide (150 μl/well) and were quantified spectroscopically at 560 nm using a SpectraMax® 190 spectrophotometer.

2.10. Western blot analysis

Ventricular tissues or isolated cardiomyocytes were homogenized and sonicated in RIPA buffer containing 20 mM Tris (pH 7.4), 150 mM NaCl, 1 mM EDTA, 1 mM EGTA, 1% Triton, 0.1% sodium dodecyl sulfate (SDS), and a protease inhibitor cocktail (Roche Diagnostics, Indianapolis, IN). Tissue or cell homogenates were resolved in SDS-polyacrylamide gels in a mini-gel apparatus (Mini-PROTEAN II, Bio-Rad, Hercules, CA) and proteins were transferred onto nitrocellulose membranes, incubated overnight with various primary antibodies at 4 °C. Membranes were incubated with horseradish peroxidase (HRP)-coupled secondary antibody for 1 h at room temperature. Signal was detected quantified with a Bio-Rad Calibrated Densitometer and the intensity of immunoblot bands was normalized to that of GAPDH. For reprobing, membranes were tripped with 50 mM Tris-HCl, 2% SDS and 0.1 M β-mercaptoethanol. Antibodies against ALDH2 (OriGene, TP300505), 4-hydroxy-2-nonenal (HNE) product adducts (Cayman, #32100), the antioxidant glutathione peroxidase (GPx2, Novus, #496010), superoxide dismutase (SOD, Sigma, S9549), TNFα (SCBT, sc-133192), IL-6 (Cell Signaling, 12912), BIP (Cell Signaling, #3183), GADD153 (SCBT, sc-7351), IRE (Abcam, ab37073), phosphorylated IRE (pIRE, Ser^{724}, Abcam48187), eIF2α (Cell Signaling, 9722), phosphorylated eIF2α (p-eIF2α, Ser^{51}, Cell Signaling, 9721), LC3B (Cell Signaling, 2775), Atg5 (Cell Signaling, 2630), p62 (Cell Signaling, 5114), Pink1 (Cell Signaling, 6946), Parkin (Cell Signaling, 2132), cleaved Caspase-3 (SCBT, sc-7272), Bax (Cell Signaling, 2772), RAB4 (Cell Signaling, 2167), RAB5a (Novus Biologicals, NB120-13253), RAB7 (Cell Signaling, 9367S), RAB9 (Cell Signaling, 5133), CaMKKβ (SCBT, sc-271674), AMPK (Cell Signaling, 2532), phosphorylated AMPK (p-AMPK, Thr^{172}, Cell Signaling, 2535), mTOR (Cell Signaling, 2972), phosphorylated mTOR (p-mTOR, Ser^{2448}, Cell Signaling, 2971), SERCA2a (Abcam 2861), and GAPDH (Cell Signaling Technology, Danvers, MA) were employed for immunoblotting [14].

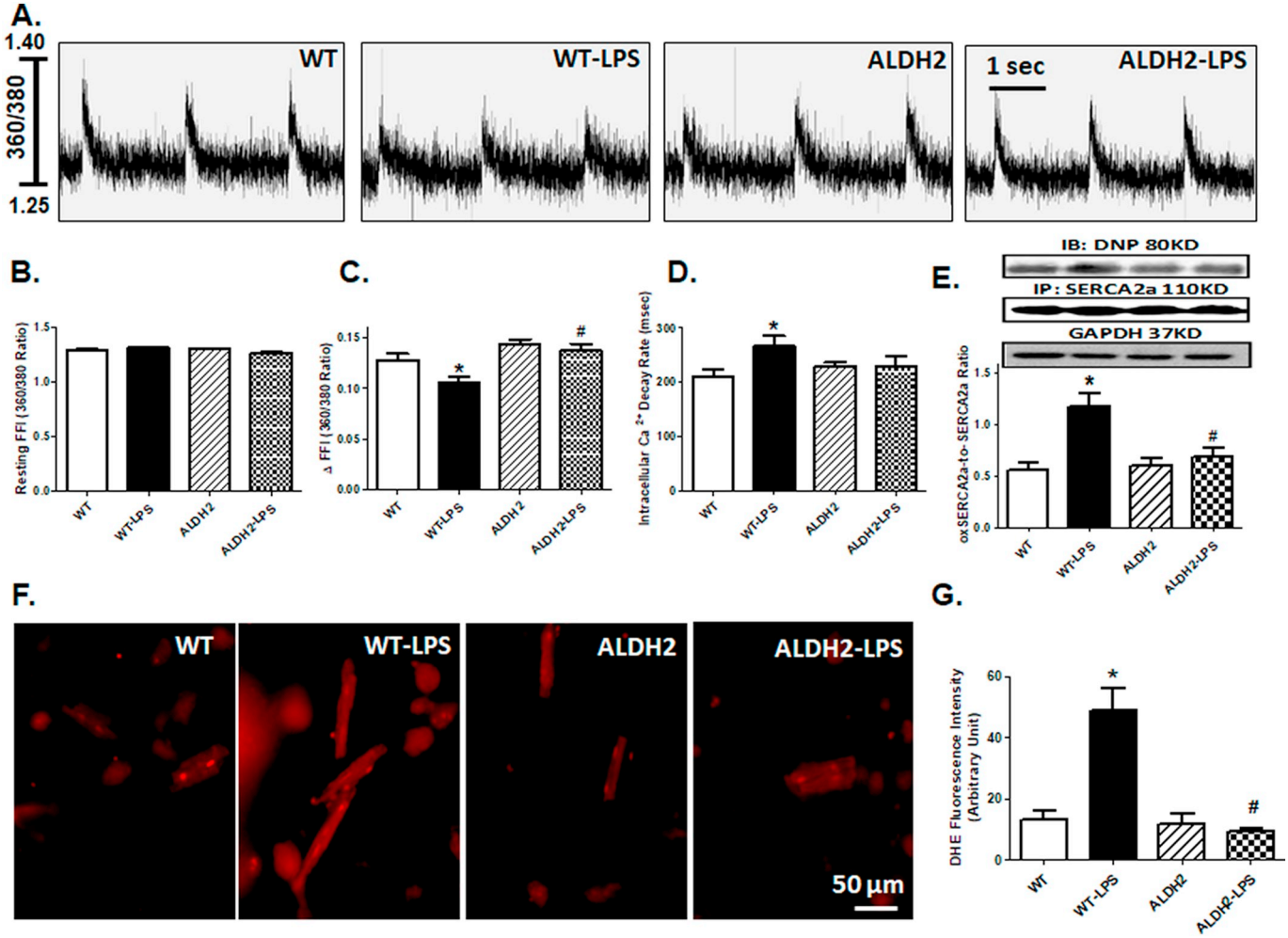

Fig. 3. Intracellular Ca^{2+} properties, SERCA oxidation and superoxide production in cardiomyocytes from WT and ALDH2 transgenic mice treated with or without LPS (4 mg/kg, i.p. for 6 h). A: Representative intracellular Ca^{2+} transients from all 4 mouse groups; B: resting Fura-2 fluorescence intensity (FFI); C: electrically-stimulated rise in FFI (ΔFFI); D: intracellular Ca^{2+} decay rate; E: oxidized and total levels of SERCA2a. Insets: Representative gel blots depicting levels of DNP and SERCA2a (GAPDH as loading control); F: representative intracellular fluorescent images depicting O_2^- levels using DHE staining in 4 experimental groups; and G: pooled data for O_2^- production. Mean ± SEM, n = 89–93 cells from 6 mice per group for pane B–D, n = 6–7 hearts for panel E, and n = 10–11 images for panel G. *$p < 0.05$ *vs.* WT group, #$p < 0.05$ *vs.* WT-LPS group.

2.11. SERCA2a oxidation

Heart tissues or cardiomyocytes were sonicated and solubilized in a buffer containing 0.5% CHAPS, 10 mM Tris-HCl, 50 mM dithiothreitol, 0.3 M sucrose at 4 °C. After centrifugation, samples were incubated with an anti-SERCA2a antibody (Abcam 2861) overnight at 4 °C. An IgG-agarose slurry was added and rotary mixed at 4 °C for 2 h. Oxidized SERCA2a was probed immunochemically using an anti-dinitrophenyl (DNP) antibody (Sigma, D9656) after derivatization with dinitrophenylhydrazine. Total SERCA2a expression after immunoprecipitation was used to normalize protein loading [38].

2.12. LC3B-GFP-adenoviral transfection in H9C2 cells

Given the poor transfection efficacy and relatively short duration of survival for murine cardiomyocytes, H9c2 cells, a clonal cell line derived from fetal rat hearts, were purchased from the American Type Culture Collection (ATCC, CRL-1446™, Manassas, VA), to assess autophagy using GFP fluorescence. Cells were grown to 80% confluence before use. Adenovirus containing the GFP-LC3 construct (provided by Dr. Cindy Miranti from University of Arizona, Phoenix, AZ) was propagated using the HEK293 cell line. Cells were transfected with GFP-LC3 adenovirus as described [48]. Upon plaque formation, infected cells were collected, washed with PBS, resuspended in culture medium, and lysed by three cycles of freeze-thaw (37 °C). Cell debris was collected by centrifugation and aliquots of supernatant with viral particles were stored at −80 °C. Adenovirus was purified using an Adeno-X Maxi purification kit (631533, Clontech Laboratories, Mountain View, CA). H9c2 cells were grown to confluence on Lab-Tek chamber slides. Cells were then infected at an MOI of 2 with adenoviruses expressing the GFP-LC3 fusion protein. Medium was replaced with fresh DMEM after 6 h. Twenty-four hours later, H9c2 cells were incubated with LPS (4 μg/ml) [16] or tunicamycin (3 μg/ml) [44] in the presence or absence of Alda-1 (20 μM) [21] or the AMPK inducer AICAR (500 μM) [41] prior to visualization of autophagy using fluorescence microscopy.

2.13. Data analysis

Data were expressed as mean ± SEM. Statistical significance ($p < 0.05$) was estimated by multi-analysis of variance followed by a Tukey's test for *post hoc* analysis. All statistics was performed with GraphPad Prism 4.0 software (GraphPad, San Diego, CA).

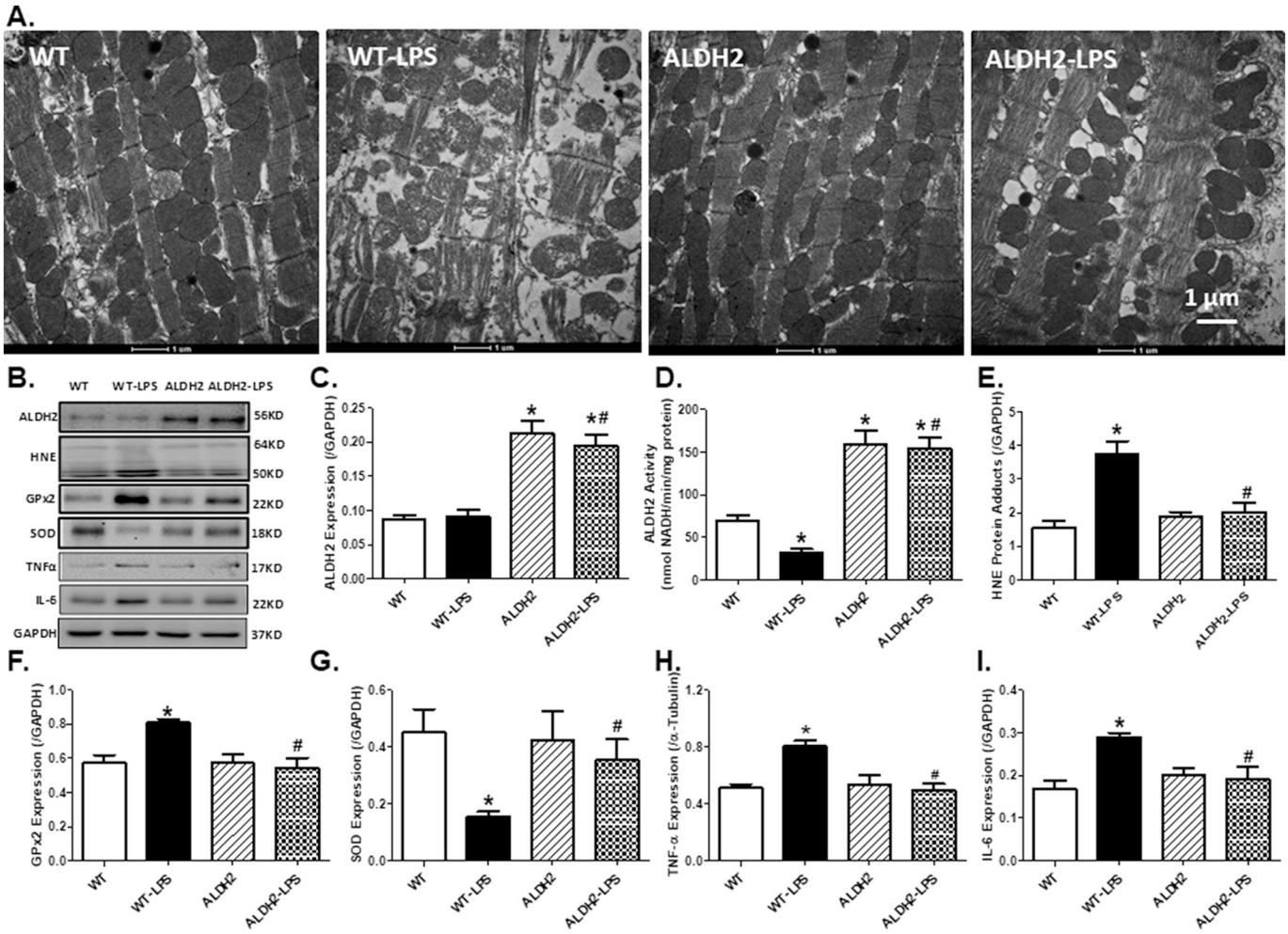

Fig. 4. Effect of LPS on ultrastructure, ALDH2, antioxidant and pro-inflammatory protein markers in hearts from WT and ALDH2 transgenic mice challenged with or without LPS (4 mg/kg, i.p. for 6 h). A: Mitochondria and sarcomere ultrastructure assessed using transmission electron microscopy in all 4 experimental groups; B: representative gel blots depicting levels of ALDH2, HNE, GPx2, SOD, TNFα and IL6 (GAPDH as loading control); C: ALDH2 levels; D: ALDH2 activity; E: HNE levels; F: GPx2 levels; G: SOD levels; H: TNFα levels; and I: IL-6 levels. Mean ± SEM, n = 6–8 mice per group, *p < 0.05 *vs.* WT group, #p < 0.05 *vs.* WT-LPS group.

3. Results

3.1. ALDH2 attenuated LPS-induced changes in myocardial echocardiographic properties

LPS challenge did not overtly affect body or heart weight in either WT or ALDH2 mice. Echocardiographic evaluation revealed that LPS challenge significantly increased left ventricular end systolic diameter (LVESD) and decreased fractional shortening in WT mice consistent with previous findings [17,49]. Although ALDH2 transgene did not affect LVESD or fractional shortening, it abrogated LPS-induced changes in echocardiographic properties. Neither LPS challenge nor ALDH2 transgene, or both, altered LV posterior wall thickness during diastole (LVPWd) or systole (LVPWs, data not shown), septal thickness, left ventricular end diastolic diameter (LVEDD) and heart rate (Fig. 1).

3.2. ALDH2 ameliorated LPS-induced cardiomyocyte contractile and intracellular Ca^{2+} defects

Consistent with echocardiographic findings, LPS markedly suppressed cardiomyocyte contractile function, as manifested by decreased peak shortening (PS) and maximal velocity of shortening/relengthening (± dL/dt), as well as prolonged TR_{90} without any change in resting cell length and TPS. ALDH2 transgene ameliorated LPS-induced cardiomyocyte contractile anomalies without any effect itself (Fig. 2). To explore the possible mechanisms behind ALDH2-offered protection against LPS exposure-induced cardiac dysfunction, intracellular Ca^{2+} handling was evaluated using the Fura-2 fluorescence microscopy. Cardiomyocytes displayed overtly decreased intracellular Ca^{2+} release in response to electrical stimuli (ΔFFI) and prolonged intracellular Ca^{2+} decay with unchanged resting intracellular Ca^{2+} (resting FFI) following LPS treatment. ALDH2 effectively reconciled LPS-induced changes in intracellular Ca^{2+} handling properties with little effect by itself (Fig. 3A–D). Assessment of intracellular Ca^{2+} handling protein SERCA revealed that LPS overtly increased SERCA oxidation without affecting its pan protein expression, the effect of which was reversed by ALDH2 with little effect from the transgene itself (Fig. 3E).

3.3. ALDH2 ameliorated LPS-induced intracellular superoxide production, ultrastructural changes, oxidant levels and inflammation

Our further study revealed that LPS challenge promoted intracellular superoxide (O_2^-) production as evidenced by DHE staining. ALDH2 obliterated LPS-induced changes in O_2^- production without any effect by itself (Fig. 3F–G). Transmission electronic microscopy (TEM) was used to evaluate the ultrastructure of sarcomere and mitochondria. Our data presented in Fig. 4A depicted pronounced cytoarchitectural aberrations such as disrupted mitochondria, distortion of sarcomeres and myofilaments in LPS-challenged myocardium, the response was largely attenuated by ALDH2 without notable

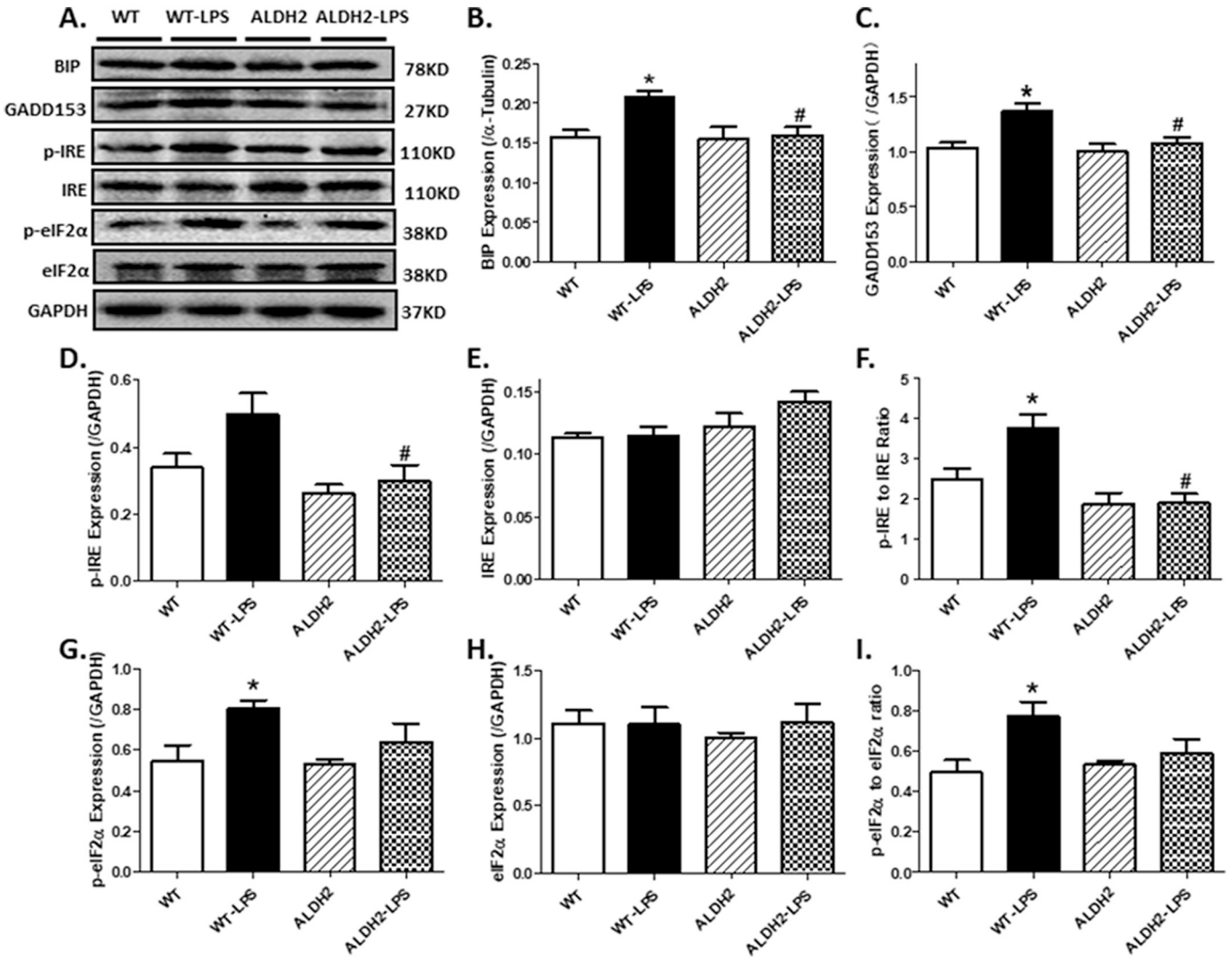

Fig. 5. ER stress markers in hearts from WT and ADLH2 mice treated with or without LPS (4 mg/kg, i.p. for 6 h). A: Representative gel blots depicting levels of the ER stress markers (GAPDH used as loading control); B: BIP; C: GADD153; D: p-IRE; E: IRE; F: p-IRE to IRE ratio; G: p-eIF2α; H: eIF2α; and I: p-eIF2α to eIF2α ratio. Mean ± SEM, n = 5–6 mice per group, *p < 0.05 *vs.* WT group; #p < 0.05 *vs.* WT-LPS group.

ultrastructural change from ALDH2 transgene itself. To examine the potential mechanism of action behind ALDH2-offered beneficial effects against LPS-induced myocardial injury, we went on to evaluate the levels and activity of ALDH2, the ALDH2 substrate 4-hydroxy-2-nonenal (HNE) protein adducts, antioxidant glutathione peroxidase (GPx2) and superoxide dismutase (SOD) as well as proinflammatory protein markers TNFα and IL-6. Our data suggested that LPS exposure significantly suppressed activity but not protein levels of ALDH2, up-regulated levels of HNE product adducts, GPx2, TNF-α and IL-6 while downregulating that of SOD, the effects of which were negated by ALDH2. ALDH2 transgene overtly increased ALDH2 protein levels and enzyme activity without affecting the levels of HNE protein adducts, GPx2, SOD, TNF-α and IL-6 (Fig. 4B–I).

3.4. Effect of ALDH2 overexpression on LPS-induced myocardial ER stress response

As shown in Fig. 5, our western blot analysis demonstrated that LPS treatment induced a robust ER stress response as evidenced by rises in ER stress protein markers including BIP, GADD153, phosphorylation of IRE and eIF2α, the effect of which was attenuated by ALDH2 over-expression. ALDH2 transgene itself did not affect ER stress itself.

3.5. Effect of ALDH2 transgene on LPS-induced myocardial autophagy, mitophagy and apoptosis

To detect autophagy, Parkin-dependent mitophagy and apoptosis, levels of autophagy, mitophagy and apoptosis protein markers LC3B, Atg5, p62, Pink1, Parkin, Bax and cleaved Caspase-3 as well as Capase-3 activity were evaluated. Our results showed that LPS challenge triggered an overt increase in LC3B II, LC3B II to LC3B I ratio, Atg5, p62, Pink1, Parkin, Bax, and cleaved Capase-3 protein levels as well as Caspase-3 activity, the effects of which were nullified by ALDH2. ALDH2 itself did not affect autophagy or apoptosis (Fig. 6).

3.6. Effect of ALDH2 transgene on LPS-induced endosomal formation and cell death

To detect endosomal formation (participating in ER tabulation, ER contacts with other organelles, membrane trafficking among Golgi complex, and autophagosome formation [35]), overall cell death and survival, levels of endosomal formation and cardiomyocyte injury were examined using the early endosomal markers RAB4 and RAB5a, the late endosomal markers RAB7 and RAB9, MTT assay and serum LDH assay. Our results showed that LPS challenge triggered a rise in RAB4, RAB5a and serum LDH levels along with decreased levels of RAB7, RAB9 and

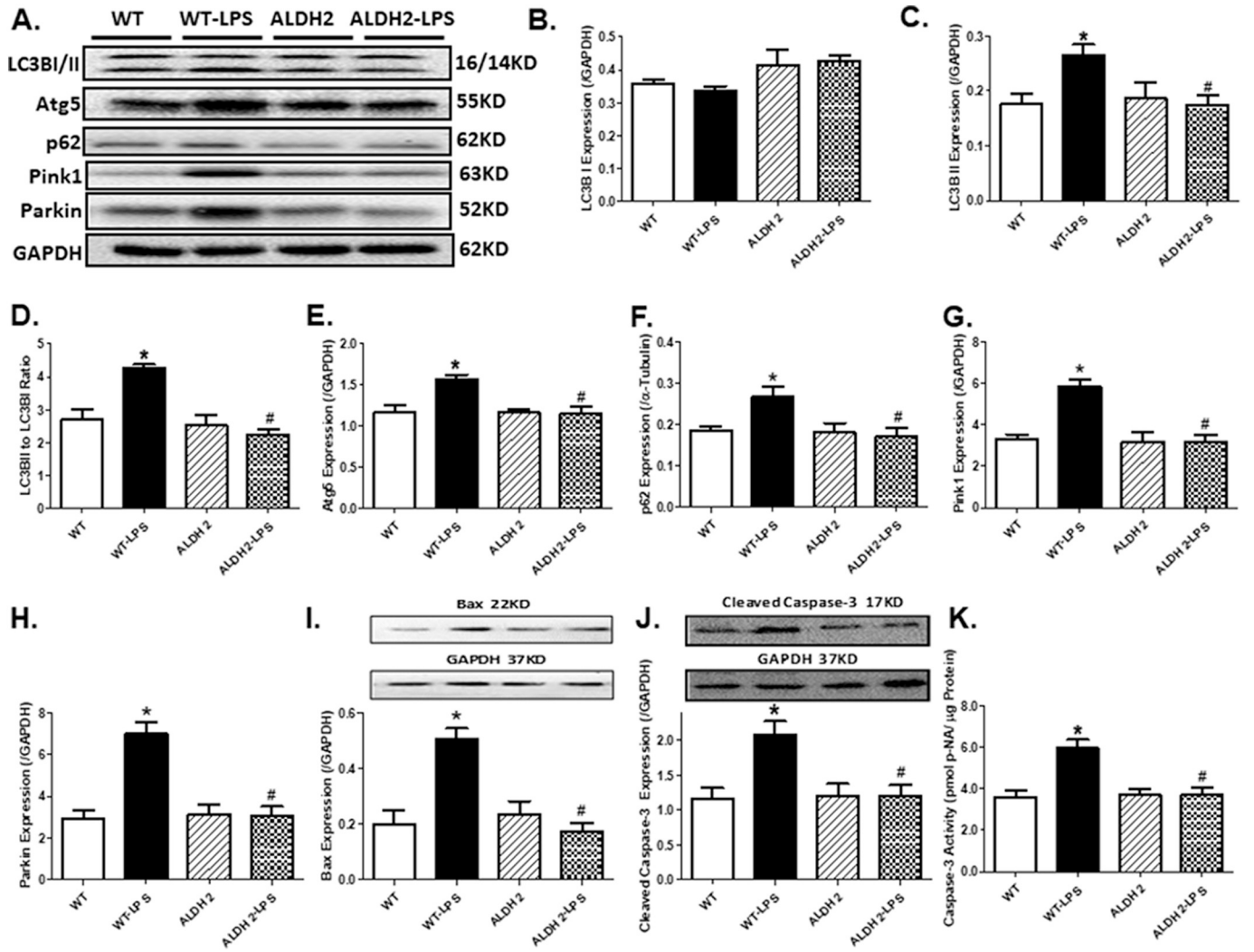

Fig. 6. Autophagy, mitophagy and apoptosis markers in hearts from WT and ALDH2 mice treated with or without LPS (4 mg/kg, i.p. for 6 h). A: Representative gel blots depicting levels of the autophagy and mitophagy markers (GAPDH used as loading control); B: LC3B I; C: LC3B II; D: LC3B II to LC3B I ratio; E: Atg5; F: p62; G: Pink1; H: Parkin; I: Bax; J: cleaved Caspase-3, insets: Representative gel blots depicting Bax and Caspase-3 (GAPDH as loading control) using specific antibodies; and K: Caspase-3 activity assay using caspase-3 colorimetric substrate (Ac-DEVD-pNA). Mean ± SEM, n = 5–6 mice per group, *p < 0.05 *vs.* WT group; #p < 0.05 *vs.* WT-LPS group.

MTT cell survival rate, the effects of which were rescued by ALDH2. ALDH2 itself did not affect endosome formation or cell death (Fig. 7).

3.7. Effect of ALDH2 on LPS-induced changes in AMPK, mTOR and CaMKKβ signaling

To explore the possible mechanisms behind LPS- and ALDH2-induced autophagy and contractile response, the essential autophagy regulatory signaling cascade AMPK/mTOR [50,51] was examined. Western blot analysis showed that LPS challenge significantly increased phosphorylation of AMPK while depressing the phosphorylation ratio of mTOR, the effect of which was negated by ALDH2. In an effort to seek regulatory factors linking ER stress and AMPK signaling, level of CaMKKβ, a downstream factor of UPR [32,33] and an upstream regulator of AMPK [31], was scrutinized. Our data revealed that LPS upregulated CaMKKβ levels, the effect of which was ameliorated by ALDH2 with little effect from ALDH2 itself (Fig. 8). These data supported the notion that LPS promotes ER stress to trigger CaMKKβ-AMPK-mTOR-mediated autophagy, the effect of which was interrupted by ALDH2.

3.8. Role of ER stress, CAMKKβ, AMPK and autophagy in ALDH2-offered protection against LPS-induced cell stress and mechanical dysfunction

In vitro study was performed to examine the effect of LPS on cardiomyocyte function and various cell stress in the absence or presence of the ALDH2 activator Alda-1 (20 μM), the ER chaperone TUDCA (500 μM), the CAMKKβ inhibitor STO-609 (5 μg/ml), or the AMPK inhibitor compound C (10 μM), or the autophagosome formation inhibitor 3-methyladenine (3-MA, 10 mM). A cohort of cardiomyocytes was treated with LPS and the ALDH2 activator alda-1 in the absence or presence of the mTOR inhibitor rapamycin (5 μM) or the AMPK inducer AICAR (500 μM) to monitor the mechanical function. Our data revealed that LPS exposure triggered overt ER stress, the effect of which was reconciled by Alda-1 and TUDCA but not STO-609, Compound C or 3-MA (Fig. 9A). However, LPS-induced rise in CAMKKβ was rescued by Alda-1, TUDCA and STO-609 but not Compound C or 3-MA (Fig. 9B). Furthermore, LPS-induced SERCA oxidation was obliterated by all pharmacological agents tested (Alda-1, TUDCA, STO-609, Compound C and 3-MA) (Fig. 9C). Pan protein expression of SERCA2a was unaffected by LPS nor any of the pharmacological agents (Fig. 9D). These discrepancies favored that CAMKKβ might occur upstream of oxidative stress albeit downstream of ER stress. Our data revealed that LPS

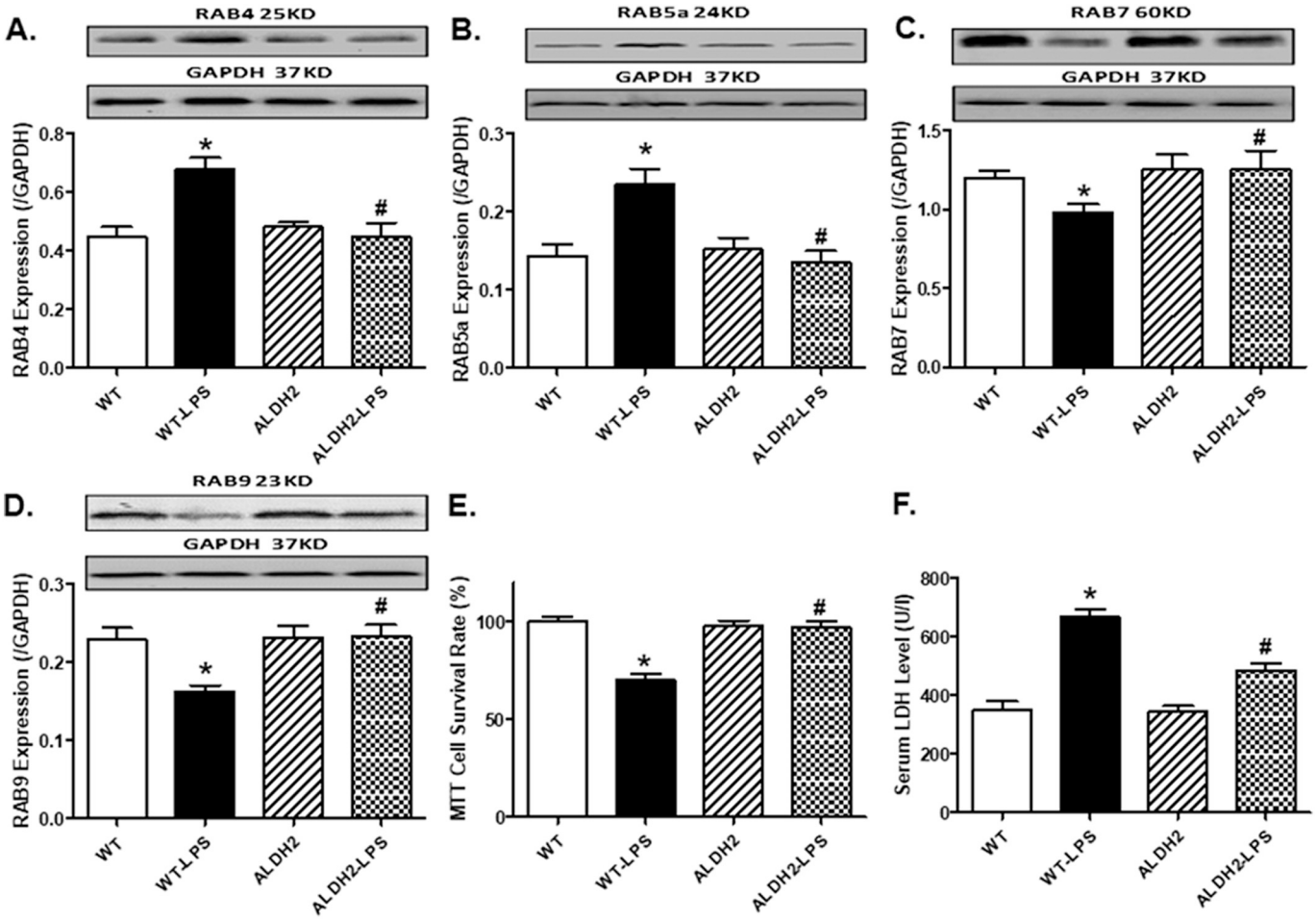

Fig. 7. Early and late endosomal markers and cell death in hearts from WT and ADLH2 mice treated with LPS (4 mg/kg, i.p. for 6 h). A: RAB4; B: RAB5A; C: RAB7; D: RAB9; insets: Representative gel blots depicting early endosomal markers RAB4 and RAB5 as well as the late endosomal markers RAB7 and RAB9 (GAPDH used as loading control); E: cell survival assay using MTT assay; and F: serum LDH levels (indicative of cardiomyocyte cell death). Mean ± SEM, n = 6–7 mice per group, *p < 0.05 *vs.* WT group; #p < 0.05 *vs.* WT-LPS group.

exposure significantly decreased peak shortening, ± dL/dt and prolonged TR_{90} without affecting TPS, the effect of which was abolished by alda-1, 3-MA or Compound C. However, the beneficial effect of alda-1 was negated by the mTOR inhibitor rapamycin and the AMPK inducer AICAR (Fig. 9E–J). Our data suggested that treatment of Alda-1 (20 μM) increased ALDH2 activity by approximately 75% in cardiomyocytes from WT mice although such effect was essentially masked by ALDH2 transgene (Supplemental Fig. S1).

3.9. Effect of ALDH2 and autophagy inhibition on ER stress-induced cardiomyocyte dysfunction

To discern the correlation between ER stress and autophagy in ALDH2-offered beneficial effect against LPS, effect of the ER stress inducer tunicamycin on cardiomyocyte contractile function was examined in the absence or presence of the autophagy inhibitor 3-MA (10 mM), the ALDH2 activator Alda-1 (20 μM), or the autophagy inducer rapamycin (5 μM). Our observations revealed that tunicamycin incubation significantly decreased peak shortening, ± dL/dt and prolonged TR_{90} without affecting resting cell length and TPS, the effects of which were ameliorated by 3-MA or Alda-1. Interestingly, the beneficial effect of Alda-1 was ablated by the autophagy inducer rapamycin (Fig. 10).

3.10. Effect of Alda-1 and autophagy induction on LPS-/ER stress-induced proinflammatory cytokine expression

To better understand the correlation among ER stress, autophagy and inflammation in LPS-induced cellular responses, isolated cardiomyocytes from WT mice were incubated with LPS (4 μg/ml) for 4 h in the absence or presence of the ALDH2 activator Alda-1 (20 μM) or tunicamycin (3 μg/ml) in the presence or absence of the autophagy inducer rapamycin (5 μM) prior to the assessment of the proinflammatory cytokine IL-6. Our data shown in Fig. S2 revealed that LPS and tunicamycin upregulated the levels of IL-6, the effects of which were ablated by Alda-1 treatment. Interestingly, induction of autophagy using rapamycin nullified Alda-1-offered beneficial effect against LPS- or ER stress-induced upregulation of IL-6. These data favored a possible downstream role for inflammation in LPS- and ALDH2-induced responses in ER stress and autophagy.

3.11. Effect of activation of ALDH2 and AMPK on LPS or ER stress-induced autophagosome accumulation in H9c2 cells

To determine if LPS-induced rise in autophagosome accumulation was due to changes in ER stress and AMPK, H9c2 myoblasts were transfected with an adenovirus expressing GFP-LC3 fusion protein for 24 h prior to exposure of LPS (4 μg/ml) or the ER stress inducer tunicamycin (3 μg/ml) for 4 h, in the absence or presence of the ALDH2 activator Alda-1 (20 μM) or the AMPK activator AICAR (500 μM). Data

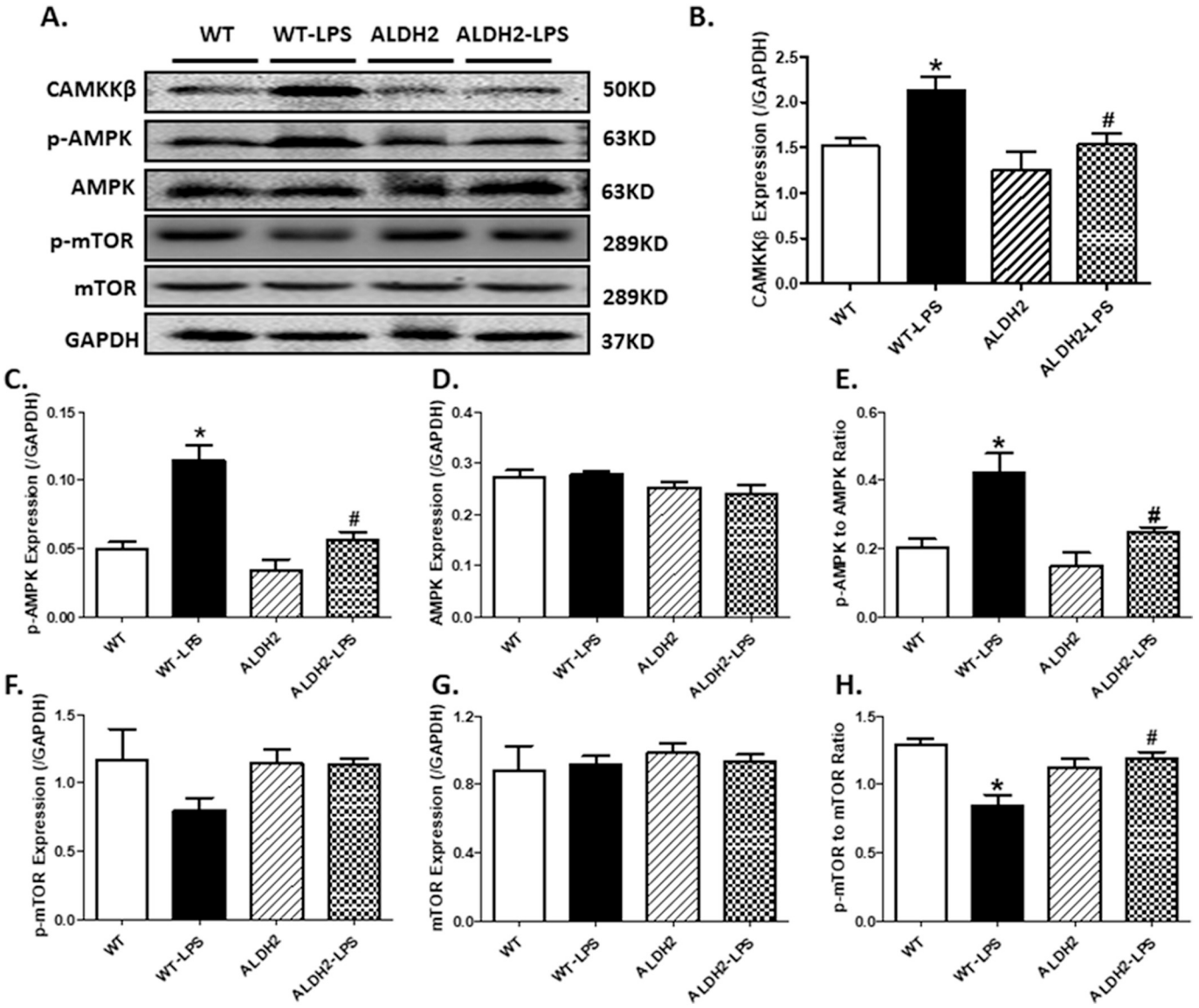

Fig. 8. Autophagy regulatory signaling in hearts from WT and ADLH2 mice treated with LPS (4 mg/kg, i.p. for 6 h). A: Representative gel blots depicting levels of CAMKKβ, pan and phosphorylated AMPK and mTOR (GAPDH used as loading control); B: CaMKKβ; C: p-AMPK; D: AMPK; E: p-AMPK to AMPK ratio; F: p-mTOR; G: mTOR; and H: p-mTOR to mTOR ratio. Mean ± SEM, n = 6 mice per group, *p < 0.05 *vs.* WT group; #p < 0.05 *vs.* WT-LPS group.

in Fig. 11 revealed that LPS significantly promoted autophagosome formation, the effect of which was abrogated by Alda-1. Interestingly, stimulation of AMPK using AICAR nullified the Alda-1-conferred protection against LPS without eliciting any effect itself. In addition, tunicamycin mimicked LPS-induced autophagosome formation, the effect of which was ablated by Alda-1. These data indicate a key role for autophagosome formation in ALDH2-induced protection against LPS–elicited change in autophagy.

4. Discussion

Although earlier findings from our lab has depicted a beneficial role for antioxidants and ER chaperone in septic cardiomyopathy [16,17], the interplay between oxidative stress and ER stress still remains elusive. In particular, antioxidant therapy failed to rescue altered autophagy and inflammation in septic hearts [16]. The salient findings from our present study revealed that ALDH2 protected against endotoxemia-induced cardiac injury possibly through ER stress-CaMKKβ/AMPK/mTOR-mediated regulation of autophagy, resulting in lessened production of intracellular O_2^- and HNE protein adducts along with changes in anti-oxidants, SERCA oxidation, necrosis, apoptosis and inflammation. LPS challenge resulted in echocardiographic and ultrastructural abnormalities (consistent with overt necrosis/apoptosis), cardiomyocyte contractile dysfunction, and intracellular Ca^{2+} mishandling, the effects of which were ameliorated by ALDH2. *In vitro* studies revealed that inhibition of autophagy using 3-MA or AMPK inhibitor compound C effectively disengaged LPS-induced detrimental mechanical and proinflammatory effects as well as SERCA oxidation (but not ER stress or CAMKKβ elevation), in a manner reminiscent of Alda-1. On the other hand, AMPK nullified ALDH2-induced benefit against LPS-induced cardiac dysfunction and autophagosome formation. These data favored a unique role for ALDH2 in obliterating LPS-induced cardiac injury *via* suppression of ER stress, early endosomes, and CaMKKβ/AMPK/mTOR-mediated autophagy excess. Our findings depicted an anti-inflammatory, anti-apoptotic, anti-necrotic and anti-oxidant responses likely downstream of ER stress and autophagy in ALDH2-offered cardiac benefits in endotoxemia (depicted in Fig. 12). These findings collectively suggested a therapeutic potential of ALDH2 in septic heart injury and indicated the potential clinical relevance of ALDH2 mutation in the setting of septic cardiomyopathy.

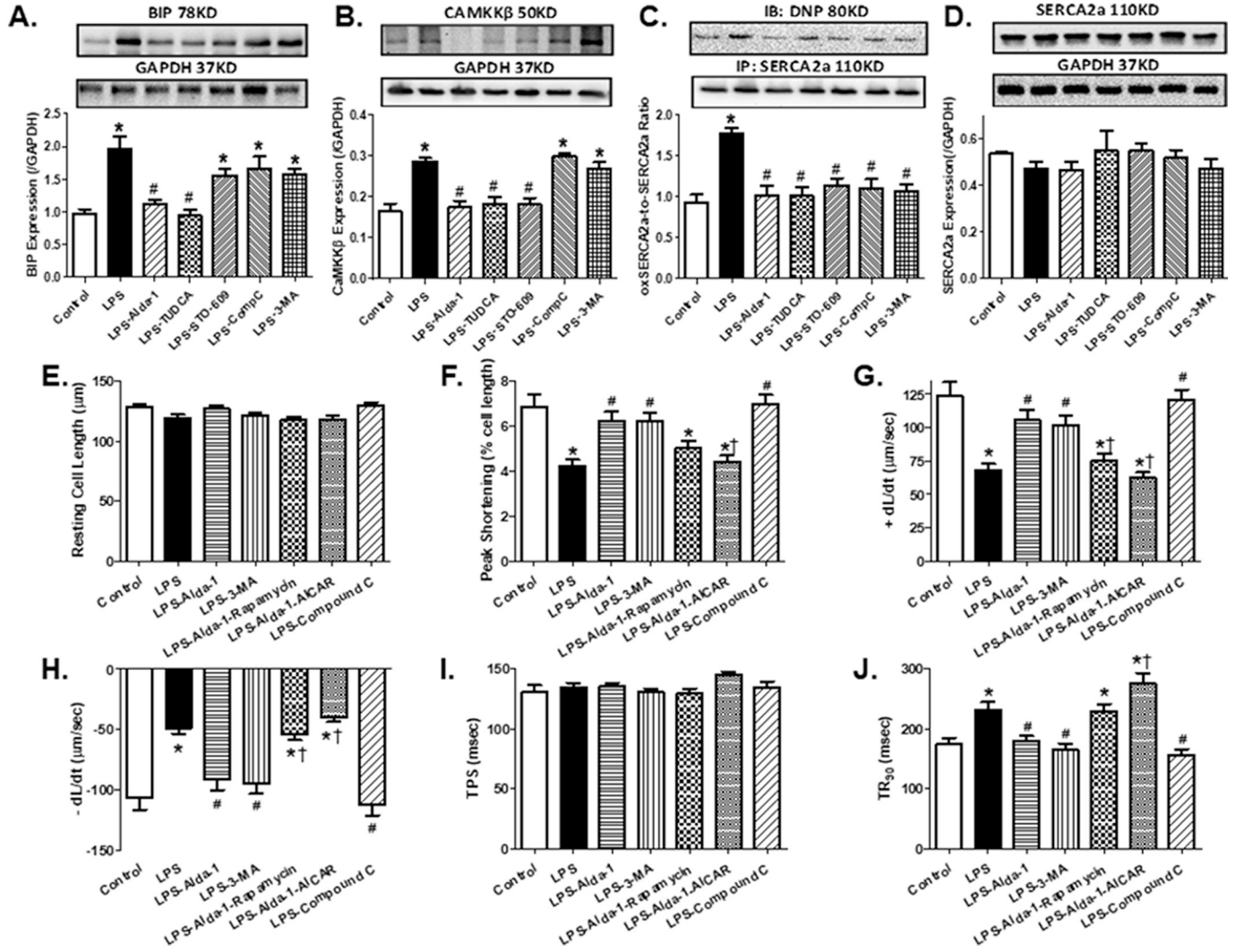

Fig. 9. Role of CAMKKβ, AMPK and autophagy in ALDH2-offered protection against LPS-induced changes in ER stress, CAMKKβ, SERCA oxidation and cardiac function. Isolated cardiomyocytes from WT mice were incubated with LPS (4 μg/ml) for 4 h in the absence or presence of the ALDH2 activator Alda-1 (20 μM), the CAMKKβ inhibitor STO-609 (5 μg/ml), the ER chaperone TUDCA (500 μM), the autophagy inhibitor 3-methlyadenine (3-MA, 10 mM), the mTOR inhibitor rapamycin (5 μM), the AMPK inducer AICAR (500 μM), or the AMPK inhibitor compound C (10 μM) prior to the assessment of protein expression or mechanical properties. A: ER stress assessed using BIP; B: CAMKKβ levels; C: oxidation of SERCA2a (using DNP) normalized to SERCA2a; D: SERCA2a level; E: resting cell length; F: peak shortening (PS); G: maximal velocity of shortening (+dL/dt); H: maximal velocity of relengthening (−dL/dt); I: time-to-peak shortening (TPS); and J: time-to-90% relengthening (TR_{90}). Mean ± SEM, n = 5–6 isolations for panels A–D and 56–62 cells from 3 mice per group for panels E–J, *$p < 0.05$ *vs.* control group, #$p < 0.05$ *vs.* LPS group, †$p < 0.05$ *vs.* LPS-Alda-1 group.

Septic cardiomyopathy is featured by dampened cardiac contractility and compliance [3]. The major component of bacterial outer membrane LPS plays an important role in the onset of cardiac anomalies in sepsis [52]. Unfavorable functional changes are documented in LPS-induced murine models as manifested by overtly compromised ultrastructure, contractile function, intracellular Ca^{2+} properties and prolonged systolic/diastolic duration in the heart [36,53]. In our hands, LPS challenge led to decreased fractional shortening, enlarged LVESD, reduced peak shortening, ± dL/dt, prolonged diastolic duration, intracellular Ca^{2+} mishandling, ultrastructural disarray in myofilament and mitochondria along with unchanged LVEDD, LV wall and septal thickness. The decreased fractional shortening, enlarged LVESD, reduced peak shortening and ± dL/dt in response to LPS challenge are consistent with elevated necrosis (decreased MTT survival and elevated LDH levels) and apoptosis (Bax and Caspase-3), denoting systolic dysfunction. On the other hand, prolonged diastolic duration and intracellular Ca^{2+} mishandling support presence of diastolic dysfunction in sepsis (which may also be resulted from necrosis and apoptosis). Interestingly, ALDH2 protected against LPS-induced ultrastructural, mechanical and intracellular Ca^{2+} abnormalities, consistent with the earlier notions for a beneficial role of the mitochondrial enzyme ALDH2 in cardiac pathologies including ischemia-reperfusion injury [25], diabetic cardiomyopathy [37], obesity cardiac dysfunction [29], dilated cardiomyopathy [54] and alcoholic cardiomyopathy [55]. ALDH2 offered benefit of intracellular Ca^{2+} handling may be related to its beneficial effect against oxidative stress (such as production of HNE protein adducts and intracellular O_2^-), resulting in alleviated oxidation of SERCA and improved Ca^{2+} handling. LPS did not affect total expression of SERCA, which is supported by previous report [56]. The elevated SERCA oxidation would also favor development of intracellular Ca^{2+} mishandling and diastolic dysfunction. Of note, our earlier findings denoted a beneficial role of ALDH2 against ER stress-induced cardiac dysfunction [28], in line with our current findings. Our results revealed overtly elevated ER stress as evidenced by BIP, GADD153, p-IRE to IRE ratio, and p-eIF2α to eIF2α ratio and oxidative stress as evidenced by HNE protein adducts, O_2^- production, elevated GPx2 (a likely

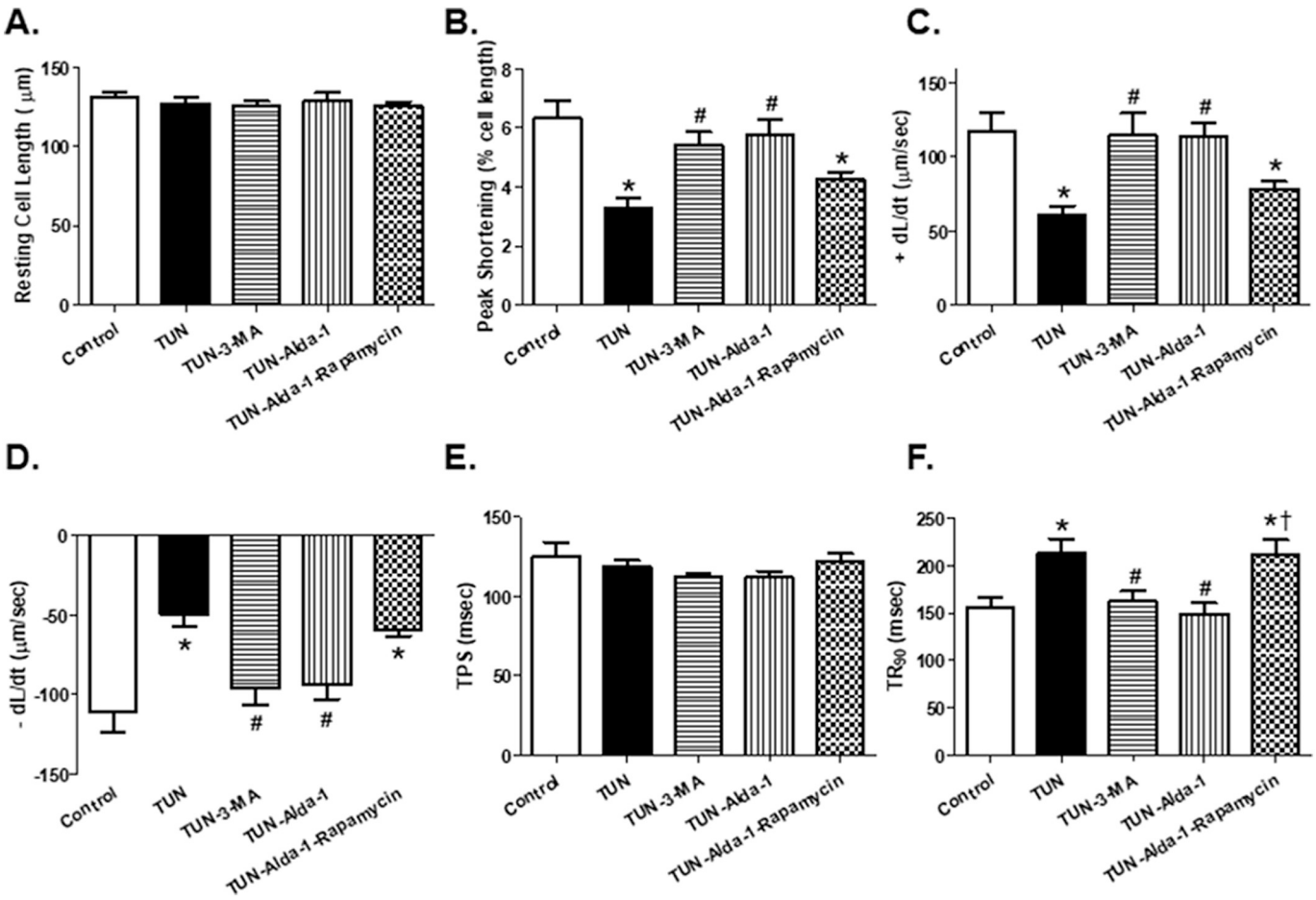

Fig. 10. Effect of ALDH2 and autophagy inhibition in ER stress-induced cardiomyocyte contractile dysfunction. Isolated cardiomyocytes from WT mice were incubated with the ER stress inducer tunicamycin (TUN, 3 μg/ml) for 4 h in the absence or presence of the autophagy inhibitor 3-MA (10 mM), the ALDH2 activator Alda-1 (20 μM) or the autophagy inducer rapamycin (5 μM) prior to the assessment of mechanical properties. A: Resting cell length; B: peak shortening (PS); C: maximal velocity of shortening (+dL/dt); D: maximal velocity of relengthening (−dL/dt); E: time-to-peak shortening (TPS); and F: time-to-90% relengthening (TR_{90}). Mean ± SEM, n = 39–43 cells per group, *p < 0.05 *vs.* control group, #p < 0.05 *vs.* TUN group, †p < 0.05 *vs.* TUN-Alda-1 group.

compensatory response) and decreased SOD levels following LPS challenge. IRE1, PERK and ATF6 comprise the three main branches for ER stress. IRE1 promotes apoptosis and autophagy through ERK/JNK pathway, while PERK activation enhances anti-oxidative proteins and pro-apoptotic proteins through the signal eIF2α. Our data confirmed changes in anti-oxidative proteins GPx2 and SOD, as well as the pro-apoptotic Bax and Caspase-3, supporting the ALDH2- and LPS-induced overall necrosis and apoptosis presentation. AFT6, on the other hand, is directly related to lipid metabolism. BIP serves as an upstream ER chaperone to turn on all three players IRE1, PERK and ATF6. GADD153 is a downstream protein of ER stress closely related to apoptosis. Our results favored IRE1 and eIF2α as the main ER stress pathways in LPS-induced endotoxemic model. ALDH2 effectively mitigated LPS-induced ER stress, suggesting a role for ER stress in ALDH2-offered benefit against endotoxemia.

Autophagy is essential to maintain cardiac homeostasis [57,58]. Our data shown in Fig. 11 suggested that autophagy served as a downstream target for Alda-1-induced responses in the face of LPS and tunicamycin challenge. This notion (as depicted in Fig. 12) also received support from mechanical findings in Figs. 9–10 where inhibition of autophagy nullified LPS- and ER stress-induced cardiomyocyte contractile dysfunction, while induction of autophagy negated Alda-1-offered beneficial effect against ER stress inducer tunicamycin. ER stress induces autophagy *via* IRE1/JNK/p38- [59,60], ATF4- [61] and Akt/mTOR- [44] mediated mechanisms. Our findings revealed a possible role for the CaMKKβ/AMPK/mTOR signaling cascade in bridging ER stress and autophagy in endotoxemia as depicted in Fig. 12. Our results noted elevated autophagy and mitophagy (Pink1-Parkin) markers and GFP-LC3 autophagosomes upon LPS challenge, which was ameliorated by ALDH2. Levels of p62, an autophagy adaptor for lysosome degradation, were elevated along with LC3B, suggesting transient accumulation of autophagosomes in the face of overwhelmed autophagy. This result was also supported by the beneficial effect of the autophagy inhibitor 3-MA, and detrimental effect of autophagy inducer rapamycin (*via* inhibition of mTOR) in cardiomyocyte function. AMPK inhibitor compound C rescued against LPS-induced cardiac contractile dysfunction but not ER stress, while the AMPK inducer AICAR or rapamycin nullified ALDH2-offered protection against LPS, favoring a role for AMPK and autophagy in ALDH2-offered beneficial effect against LPS/ER stress. CaMKKβ, an important upstream regulator of AMPK [62,63], is sensitive to Ca^{2+} abnormality in ER stress. Our data presented in Fig. 9A–B also confirmed that ER stress may serve as an upstream regulator for CaMKKβ/AMPK signaling. Earlier studies showed overtly increased CaMKKβ level in ER stress [32,64] and obese hearts [29], in line with our current findings. To this end, it is plausible to speculate that CaMKKβ serves as a springboard between ER stress and AMPK activation, ultimately resulting in excess autophagy (Fig. 12). This is consistent with our recent report that ALDH2 protects against obesity cardiomyopathy through a CaMKKβ-AMPK-mediated regulation of autophagy [29].

Data from our study revealed elevated levels of protein markers for early endosomal pathway (RAB4 and RAB5a) and decreased late endosome formation (RAB7 and RAB 9) in response to LPS challenge, the

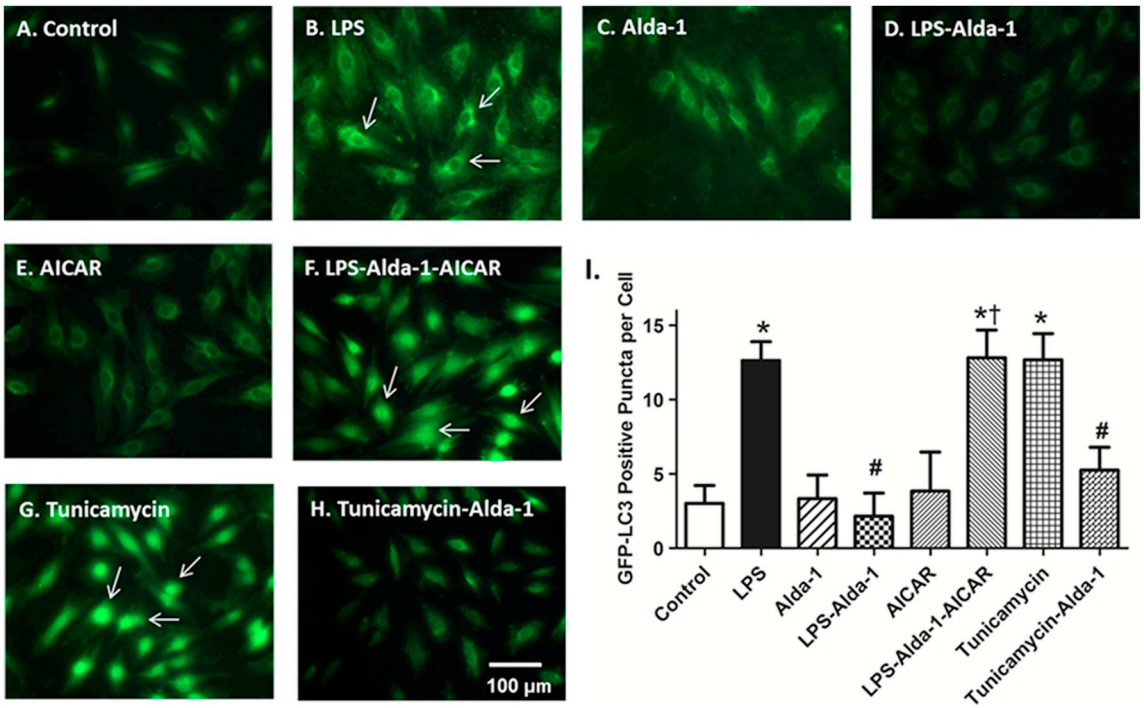

Fig. 11. Role of AMPK and ER stress in ALDH2-offered protection against LPS-induced autophagy induction. H9c2 cells were transfected with adenovirus for 24 h to express the GFP-LC3 fusion protein. Cells were then exposed to LPS (4 μg/ml) for 4 h in the absence or presence of the ALDH2 activator Alda-1 (20 μM), the AMPK activator AICAR (500 μM) the AMPK inhibitor Compound C (10 μM) or the ER stress inducer tunicamycin (3 μg/ml). A-H: Representative images depicting GFP-LC3 puncta in H9c2 cells; Arrowheads denote the GFP-LC3 autophagosomes; and I: Percentage of cells with autophagosomes. Cells with 10 + punctate spots were scored as positive for autophagosomes. Mean ± SEM, n = 6–7 images per group, *$p < 0.05$ *vs.* control group, $^{\#}p < 0.05$ *vs.* LPS or tunicamycin group, $^{\dagger}p < 0.05$ *vs.* LPS-Alda-1 group,

effect of which was ablated by ALDH2. These Ras-related small GTPases regulate ER tabulation, ER contacts, membrane trafficking among Golgi complex, endosome, and autophagosome formation [35]. Moreover, activation of Ras will target cell surface proteins for lysosomal degradation, an endocytotic event promoting both cell death (*e.g.*, apoptosis, necrosis and autophagic cell death) and cell survival, depending on factors such as relative abundance and subcellular localization of functionally distinct Ras isoforms. RAB 4 and RAB5a are vital for early endocytic pathway whereas RAB7 and RAB9 regulate late endosome transport. These small GTPases govern autophagy process and serve as the molecular 'switches' to regulate the formation, transport, tethering, and fusion of transport vesicles [34,35]. Our observation of elevated early endosome formation (RAB4 and RAB5a) supports increased autophagosome formation (LC3B, Pink1-Parkin and Beclin1) while decreased late endosome formation (RAB7 and RAB 9) supports dampened fusion with lysosomes (elevated p62) in the face of LPS challenge. These findings also provide an "endosome" connection between ER (given the nature of ER localization for Ras-related small GTPases) and autophagy.

Data from our current study also indicated that ALDH2 or Alda-1 resisted LPS-induced proinflammatory cytokines including TNFα and IL-6, consistent with the anti-inflammatory property of ALDH2 in other pathological settings [24,65,66]. It is difficult to discern the origin of these cytokines. Pro-inflammatory mediators (such as TNF-α and IL-6) are mainly secreted by monocytes and macrophages with some contributions from cardiomyocytes and endothelial cells [67,68]. Data from Fig. S2 also depicted that inflammation might serve as a downstream target for Alda-1-elicited response against LPS and ER stress. More importantly, induction of autophagy using rapamycin ablated Alda-1-induced benefits against LPS and ER stress in the level of the proinflammatory cytokine IL-6. It should be noted that ALDH2 may also elicit undesirable cardiac functional sequelae in certain conditions such as aging [69]. Although the underlying mechanism for this apparent discrepancy remains elusive, ALDH2 requires NAD^+ as its cofactor thus creating a competition with the longevity regulator Sirt1 (NAD^+-dependent) to compromise aging process. Although mitochondrial localization of ALDH2 carries detoxification capacity of aldehydes, our ALDH2 transgenic mouse model does not restrict the overexpression solely in mitochondria. Further study is needed to discern the NAD^+ requirement and intracellular localization of ALDH2 in endotoxemia.

In summary, findings from our current study help to advance the field in several ways. (1). Our data should shed some lights towards understanding the interplay among the discrete components in sepsis, namely ER stress, endosome formation, oxidative stress, autophagy and apoptosis. ALDH2 protects against LPS-induced cardiac dysfunction possibly through suppression of ER stress, early endosome formation, CAMKKβ/AMPK/mTOR pathway, and autophagy, leading to preserved mitochondrial O_2^- levels, oxidative stress (such as HNE protein adducts and SERCA oxidation) and attenuation of inflammation (Fig. 12). (2). Our findings support a beneficial role for ALDH2 in the maintenance of cardiac homeostasis in endotoxemia. Targeting ALDH2 enzyme may offer some promises in the therapeutics of sepsis and septic cardiomyopathy in particular in patients with ALDH2 mutation although further clinical validation is warranted.

Conflict of interest

None of the authors declare any potential conflict of interest.

Transparency document

The Transparency document associated with this article can be found, in online version.

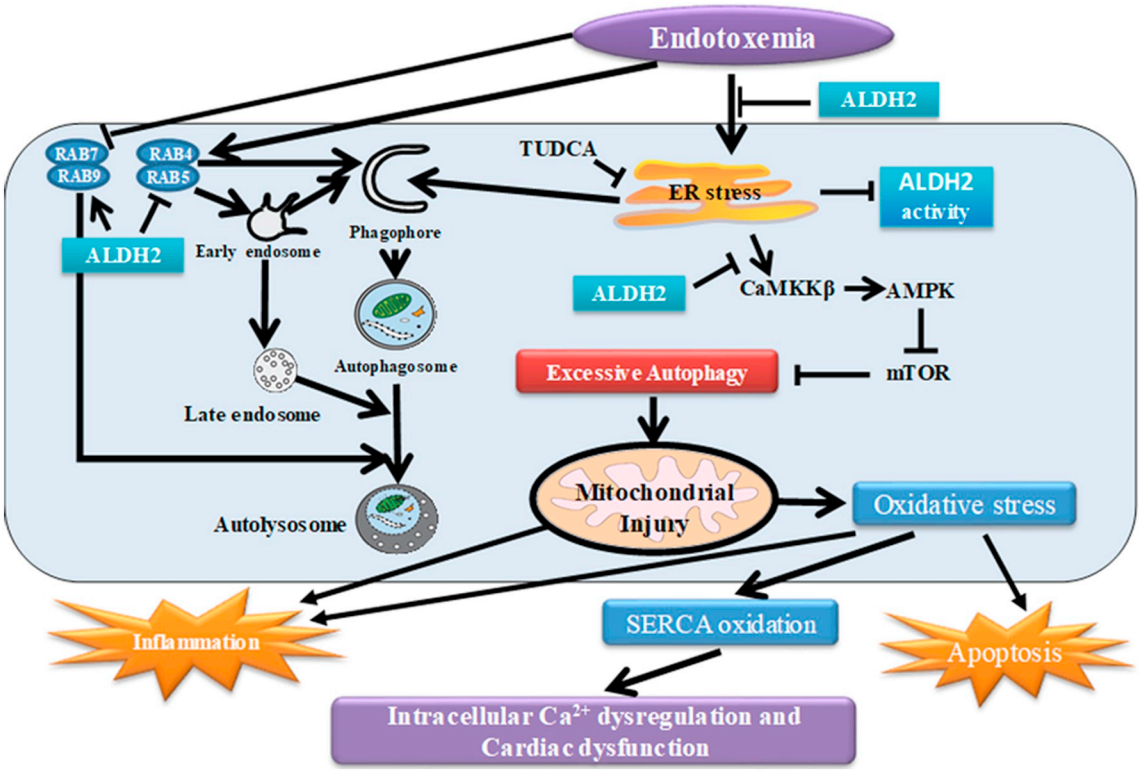

Fig. 12. Scheme depicting possible mechanism(s) involved in LPS- and ALDH2-induced changes in autophagy, early and late endosome formation, as well as cardiac contractile function. LPS triggers ER stress and suppresses ALDH2 activity, leading to activation of CaMKKβ and AMPK to suppress mTOR signaling, ultimately resulting in excess autophagy. LPS exposure also prompts oxidative stress, inflammation and mitochondrial injury, which may happen as a result of excessive autophagy. At the same time, LPS promotes early endosome formation (RAB4 and RAB5) to favor autophagosome formation while inhibiting late endosome formation (RAB7, RAB9) to retard autophagolysosome formation. ALDH2 counters ER stress, oxidative stress, inflammation, early endosome formation, and excessive autophagy to preserve mitochondrial integrity and cardiac function. Arrowheads denote stimulation whereas the lines with a "T" ending represent inhibition.

Acknowledgments

The work was supported in part by the National Institutes of Health/ National Institute of General Medical Sciences [8P20GM103432], University of Wyoming Faculty Research Fund, National Natural Science Foundation of China (81570225, 81522004, 81679138, 81501696 and 81701952) and China Scholarship Council.

Appendix A. Supplementary data

Supplementary data to this article can be found online at https://doi.org/10.1016/j.bbadis.2019.03.015.

References

[1] G.S. Martin, D.M. Mannino, S. Eaton, M. Moss, The epidemiology of sepsis in the United States from 1979 through 2000, N. Engl. J. Med. 348 (2003) 1546–1554.
[2] J. Ren, S. Wu, A burning issue: do sepsis and systemic inflammatory response syndrome (SIRS) directly contribute to cardiac dysfunction? Frontiers in Bioscience: a journal and virtual library 11 (2006) 15–22.
[3] M.W. Merx, C. Weber, Sepsis and the heart, Circulation 116 (2007) 793–802.
[4] A. Rudiger, M. Singer, Mechanisms of sepsis-induced cardiac dysfunction, Crit. Care Med. 35 (2007) 1599–1608.
[5] G. Stanzani, M.R. Duchen, M. Singer, The role of mitochondria in sepsis-induced cardiomyopathy, Biochim. Biophys. Acta Mol. basis Dis. 1865 (2019) 759–773.
[6] J.H. Maley, M.E. Mikkelsen, Short-term gains with long-term consequences, the evolving story of sepsis survivorship, Clin Chest Med 37 (2016) 367–380.
[7] P. Zhao, S. Turdi, F. Dong, X. Xiao, G. Su, X. Zhu, G.I. Scott, J. Ren, Cardiac-specific overexpression of insulin-like growth factor I (IGF-1) rescues lipopolysaccharide-induced cardiac dysfunction and activation of stress signaling in murine cardiomyocytes, Shock 32 (2009) 100–107.
[8] M.M. Khan, W.L. Yang, P. Wang, Endoplasmic reticulum stress in sepsis, Shock 44 (2015) 294–304.
[9] B. Mollereau, S. Manie, F. Napoletano, Getting the better of ER stress, J Cell Commun Signal 8 (2014) 311–321.
[10] S. Wang, X. Chen, S. Nair, D. Sun, X. Wang, J. Ren, Deletion of protein tyrosine phosphatase 1B obliterates endoplasmic reticulum stress-induced myocardial dysfunction through regulation of autophagy, Biochim. Biophys. Acta 1863 (2017) 3060–3074.
[11] Y. Liu, B. Levine, Autosis and autophagic cell death: the dark side of autophagy, Cell Death Differ. 22 (2015) 367–376.
[12] A.M. Gorman, S.J. Healy, R. Jager, A. Samali, Stress management at the ER: regulators of ER stress-induced apoptosis, Pharmacol. Ther. 134 (2012) 306–316.
[13] J. Piquereau, R. Godin, S. Deschenes, V.L. Bessi, M. Mofarrahi, S.N. Hussain, Y. Burelle, Protective role of PARK2/Parkin in sepsis-induced cardiac contractile and mitochondrial dysfunction, Autophagy 9 (2013) 1837–1851.
[14] J. Ren, X. Xu, Q. Wang, S.Y. Ren, M. Dong, Y. Zhang, Permissive role of AMPK and autophagy in adiponectin deficiency-accentuated myocardial injury and inflammation in endotoxemia, J. Mol. Cell. Cardiol. 93 (2016) 18–31.
[15] Y. Sun, X. Yao, Q.J. Zhang, M. Zhu, Z.P. Liu, B. Ci, Y. Xie, D. Carlson, B.A. Rothermel, Y. Sun, B. Levine, J.A. Hill, S.E. Wolf, J.P. Minei, Q.S. Zang, Beclin-1-dependent autophagy protects the heart during sepsis, Circulation 138 (2018) 2247–2262.
[16] A.F. Ceylan-Isik, P. Zhao, B. Zhang, X. Xiao, G. Su, J. Ren, Cardiac overexpression of metallothionein rescues cardiac contractile dysfunction and endoplasmic reticulum stress but not autophagy in sepsis, J. Mol. Cell. Cardiol. 48 (2010) 367–378.
[17] S. Turdi, X. Han, A.F. Huff, N.D. Roe, N. Hu, F. Gao, J. Ren, Cardiac-specific overexpression of catalase attenuates lipopolysaccharide-induced myocardial contractile dysfunction: role of autophagy, Free Radic. Biol. Med. 53 (2012) 1327–1338.
[18] Y. Zhang, J. Ren, ALDH2 in alcoholic heart diseases: molecular mechanism and clinical implications, Pharmacol. Ther. 132 (2011) 86–95.
[19] N. Kato, F. Takeuchi, Y. Tabara, T.N. Kelly, M.J. Go, X. Sim, W.T. Tay, C.H. Chen, Y. Zhang, K. Yamamoto, T. Katsuya, M. Yokota, Y.J. Kim, R.T. Ong, T. Nabika, D. Gu, L.C. Chang, Y. Kokubo, W. Huang, K. Ohnaka, Y. Yamori, E. Nakashima, C.E. Jaquish, J.Y. Lee, M. Seielstad, M. Isono, J.E. Hixson, Y.T. Chen, T. Miki, X. Zhou, T. Sugiyama, J.P. Jeon, J.J. Liu, R. Takayanagi, S.S. Kim, T. Aung, Y.J. Sung, X. Zhang, T.Y. Wong, B.G. Han, S. Kobayashi, T. Ogihara, D. Zhu, N. Iwai, J.Y. Wu, Y.Y. Teo, E.S. Tai, Y.S. Cho, J. He, Meta-analysis of genome-wide association studies identifies common variants associated with blood pressure variation in east Asians, Nat. Genet. 43 (2011) 531–538.
[20] Y. Zhang, C. Wang, J. Zhou, A. Sun, L.K. Hueckstaedt, J. Ge, J. Ren, Complex inhibition of autophagy by mitochondrial aldehyde dehydrogenase shortens lifespan and exacerbates cardiac aging, Biochim. Biophys. Acta 1863 (2017) 1919–1932.
[21] C.H. Chen, G.R. Budas, E.N. Churchill, M.H. Disatnik, T.D. Hurley, D. Mochly-

Rosen, Activation of aldehyde dehydrogenase-2 reduces ischemic damage to the heart, Science 321 (2008) 1493–1495.
[22] J. Pang, J. Wang, Y. Zhang, F. Xu, Y. Chen, Targeting acetaldehyde dehydrogenase 2 (ALDH2) in heart failure-recent insights and perspectives, Biochim. Biophys. Acta 1863 (2017) 1933–1941.
[23] B. Liu, J. Wang, M. Li, Q. Yuan, M. Xue, F. Xu, Y. Chen, Inhibition of ALDH2 by O-GlcNAcylation contributes to the hyperglycemic exacerbation of myocardial ischemia/reperfusion injury, Oncotarget 8 (2017) 19413–19426.
[24] C. Pan, J.H. Xing, C. Zhang, Y.M. Zhang, L.T. Zhang, S.J. Wei, M.X. Zhang, X.P. Wang, Q.H. Yuan, L. Xue, J.L. Wang, Z.Q. Cui, Y. Zhang, F. Xu, Y.G. Chen, Aldehyde dehydrogenase 2 inhibits inflammatory response and regulates atherosclerotic plaque, Oncotarget 7 (2016) 35562–35576.
[25] H. Ma, R. Guo, L. Yu, Y. Zhang, J. Ren, Aldehyde dehydrogenase 2 (ALDH2) rescues myocardial ischaemia/reperfusion injury: role of autophagy paradox and toxic aldehyde, Eur. Heart J. 32 (2011) 1025–1038.
[26] H. Ma, J. Li, F. Gao, J. Ren, Aldehyde dehydrogenase 2 ameliorates acute cardiac toxicity of ethanol, role of protein phosphatase and forkhead transcription factor, J Am Coll Cardiol 54 (2009) 2187–2196.
[27] S.Y. Li, S.A. Gilbert, Q. Li, J. Ren, Aldehyde dehydrogenase-2 (ALDH2) ameliorates chronic alcohol ingestion-induced myocardial insulin resistance and endoplasmic reticulum stress, J. Mol. Cell. Cardiol. 47 (2009) 247–255.
[28] B. Zhang, Y. Zhang, K.H. La Cour, K.L. Richmond, X.M. Wang, J. Ren, Mitochondrial aldehyde dehydrogenase obliterates endoplasmic reticulum stress-induced cardiac contractile dysfunction via correction of autophagy, Biochim. Biophys. Acta 1832 (2013) 574–584.
[29] S. Wang, C. Wang, S. Turdi, K.L. Richmond, Y. Zhang, J. Ren, ALDH2 protects against high fat diet-induced obesity cardiomyopathy and defective autophagy: role of CaM kinase II, histone H3K9 methyltransferase SUV39H, Sirt1, and PGC-1alpha deacetylation, Int. J. Obes. 42 (2018) 1073–1087.
[30] K. Tanaka, K.A. Whelan, P.M. Chandramouleeswaran, S. Kagawa, S.L. Rustgi, C. Noguchi, M. Guha, S. Srinivasan, Y. Amanuma, S. Ohashi, M. Muto, A.J. Klein-Szanto, E. Noguchi, N.G. Avadhani, H. Nakagawa, ALDH2 modulates autophagy flux to regulate acetaldehyde-mediated toxicity thresholds, Am. J. Cancer Res. 6 (2016) 781–796.
[31] X. Zhou, Y. Cao, G. Ao, L. Hu, H. Liu, J. Wu, X. Wang, M. Jin, S. Zheng, X. Zhen, N.J. Alkayed, J. Jia, J. Cheng, CaMKKbeta-dependent activation of AMP-activated protein kinase is critical to suppressive effects of hydrogen sulfide on neuroinflammation, Antioxid. Redox Signal. 21 (2014) 1741–1758.
[32] H. Xi, J.C. Barredo, J.R. Merchan, T.J. Lampidis, Endoplasmic reticulum stress induced by 2-deoxyglucose but not glucose starvation activates AMPK through CaMKKbeta leading to autophagy, Biochem. Pharmacol. 85 (2013) 1463–1477.
[33] C. Bracken, P. Beauverger, O. Duclos, R.J. Russo, K.A. Rogers, H. Husson, T.A. Natoli, S.R. Ledbetter, P. Janiak, O. Ibraghimov-Beskrovnaya, N.O. Bukanov, CaMKII as a pathological mediator of ER stress, oxidative stress, and mitochondrial dysfunction in a murine model of nephronophthisis, American Journal of Physiology. Renal Physiology 310 (2016) F1414–F1422.
[34] C. Puri, M. Vicinanza, D.C. Rubinsztein, Phagophores evolve from recycling endosomes, Autophagy 14 (2018) 1475–1477.
[35] C. Ortiz Sandoval, T. Simmen, Rab proteins of the endoplasmic reticulum: functions and interactors, Biochem. Soc. Trans. 40 (2012) 1426–1432.
[36] Y. Zhang, X. Xu, A.F. Ceylan-Isik, M. Dong, Z. Pei, Y. Li, J. Ren, Ablation of Akt2 protects against lipopolysaccharide-induced cardiac dysfunction: role of Akt ubiquitination E3 ligase TRAF6, J. Mol. Cell. Cardiol. 74 (2014) 76–87.
[37] Y. Zhang, S.A. Babcock, N. Hu, J.R. Maris, H. Wang, J. Ren, Mitochondrial aldehyde dehydrogenase (ALDH2) protects against streptozotocin-induced diabetic cardiomyopathy: role of GSK3beta and mitochondrial function, BMC Med. 10 (2012) 40.
[38] Z. Pei, Q. Deng, S.A. Babcock, E.Y. He, J. Ren, Y. Zhang, Inhibition of advanced glycation endproduct (AGE) rescues against streptozotocin-induced diabetic cardiomyopathy: role of autophagy and ER stress, Toxicol. Lett. 284 (2018) 10–20.
[39] I.J. Lee, C.W. Lee, J.H. Lee, CaMKKbeta-AMPKalpha2 signaling contributes to mitotic Golgi fragmentation and the G2/M transition in mammalian cells, Cell Cycle 14 (2015) 598–611.
[40] R. Guo, G.I. Scott, J. Ren, Involvement of AMPK in alcohol dehydrogenase accentuated myocardial dysfunction following acute ethanol challenge in mice, PLoS One 5 (2010) e11268.
[41] H.K. Nyblom, E. Sargsyan, P. Bergsten, AMP-activated protein kinase agonist dose dependently improves function and reduces apoptosis in glucotoxic beta-cells without changing triglyceride levels, J. Mol. Endocrinol. 41 (2008) 187–194.
[42] H. Yuan, C.N. Perry, C. Huang, E. Iwai-Kanai, R.S. Carreira, C.C. Glembotski, R.A. Gottlieb, LPS-induced autophagy is mediated by oxidative signaling in cardiomyocytes and is associated with cytoprotection, Am. J. Physiol. Heart Circ. Physiol. 296 (2009) H470–H479.
[43] P.O. Seglen, P.B. Gordon, 3-Methyladenine: specific inhibitor of autophagic/lysosomal protein degradation in isolated rat hepatocytes, Proc. Natl. Acad. Sci. U. S. A. 79 (1982) 1889–1892.
[44] J. Pang, N.D. Fuller, N. Hu, L.A. Barton, J.M. Henion, R. Guo, Y. Chen, J. Ren, Alcohol dehydrogenase protects against endoplasmic reticulum stress-induced myocardial contractile dysfunction via attenuation of oxidative stress and autophagy: role of PTEN-Akt-mTOR signaling, PLoS One 11 (2016) e0147322.
[45] S. Wang, W. Ge, C. Harns, X. Meng, Y. Zhang, J. Ren, Ablation of toll-like receptor 4 attenuates aging-induced myocardial remodeling and contractile dysfunction through NCoRI-HDAC1-mediated regulation of autophagy, J. Mol. Cell. Cardiol. 119 (2018) 40–50.
[46] X. Xu, Y. Hua, S. Nair, Y. Zhang, J. Ren, Akt2 knockout preserves cardiac function in high-fat diet-induced obesity by rescuing cardiac autophagosome maturation, J. Mol. Cell Biol. 5 (2013) 61–63.
[47] S. Wang, X. Zhu, L. Xiong, J. Ren, Ablation of Akt2 prevents paraquat-induced myocardial mitochondrial injury and contractile dysfunction: role of Nrf2, Toxicol. Lett. 269 (2017) 1–14.
[48] R. Guo, N. Hu, M.R. Kandadi, J. Ren, Facilitated ethanol metabolism promotes cardiomyocyte contractile dysfunction through autophagy in murine hearts, Autophagy 8 (2012) 593–608.
[49] M. Dong, N. Hu, Y. Hua, X. Xu, M.R. Kandadi, R. Guo, S. Jiang, S. Nair, D. Hu, J. Ren, Chronic Akt activation attenuated lipopolysaccharide-induced cardiac dysfunction via Akt/GSK3beta-dependent inhibition of apoptosis and ER stress, Biochim. Biophys. Acta 1832 (2013) 848–863.
[50] L. Shang, X. Wang, AMPK and mTOR coordinate the regulation of Ulk1 and mammalian autophagy initiation, Autophagy 7 (2011) 924–926.
[51] Q. Wang, L. Yang, Y. Hua, S. Nair, X. Xu, J. Ren, AMP-activated protein kinase deficiency rescues paraquat-induced cardiac contractile dysfunction through an autophagy-dependent mechanism, Toxicological Sciences: an official journal of the Society of Toxicology 142 (2014) 6–20.
[52] J.A. Nemzek, K.M. Hugunin, M.R. Opp, Modeling sepsis in the laboratory: merging sound science with animal well-being, Comp Med 58 (2008) 120–128.
[53] J. Ren, B.H. Ren, A.C. Sharma, Sepsis-induced depressed contractile function of isolated ventricular myocytes is due to altered calcium transient properties, Shock 18 (2002) 285–288.
[54] A. Sun, Y. Cheng, Y. Zhang, Q. Zhang, S. Wang, S. Tian, Y. Zou, K. Hu, J. Ren, J. Ge, Aldehyde dehydrogenase 2 ameliorates doxorubicin-induced myocardial dysfunction through detoxification of 4-HNE and suppression of autophagy, J. Mol. Cell. Cardiol. 71 (2014) 92–104.
[55] H. Ma, L. Yu, E.A. Byra, N. Hu, K. Kitagawa, K.I. Nakayama, T. Kawamoto, J. Ren, Aldehyde dehydrogenase 2 knockout accentuates ethanol-induced cardiac depression: role of protein phosphatases, J. Mol. Cell. Cardiol. 49 (2010) 322–329.
[56] I.A. Hobai, E.S. Buys, J.C. Morse, J. Edgecomb, E.H. Weiss, A.A. Armoundas, X. Hou, A.R. Khandelwal, D.A. Siwik, P. Brouckaert, R.A. Cohen, W.S. Colucci, SERCA Cys674 sulphonylation and inhibition of L-type Ca2+ influx contribute to cardiac dysfunction in endotoxemic mice, independent of cGMP synthesis, Am. J. Physiol. Heart Circ. Physiol. 305 (2013) H1189–H1200.
[57] S. Lavandero, M. Chiong, B.A. Rothermel, J.A. Hill, Autophagy in cardiovascular biology, J. Clin. Invest. 125 (2015) 55–64.
[58] J. Ren, Y. Zhang, Targeting autophagy in aging and aging-related cardiovascular diseases, Trends Pharmacol. Sci. 39 (2018) 1064–1076.
[59] J. Groenendyk, P.K. Sreenivasaiah, D.H. Kim, L.B. Agellon, M. Michalak, Biology of endoplasmic reticulum stress in the heart, Circ. Res. 107 (2010) 1185–1197.
[60] D. Brunen, M.J. Garcia-Barchino, D. Malani, N. Jagalur Basheer, C. Lieftink, R.L. Beijersbergen, A. Murumagi, K. Porkka, M. Wolf, C.M. Zwaan, M. Fornerod, O. Kallioniemi, J.A. Martinez-Climent, R. Bernards, Intrinsic resistance to PIM kinase inhibition in AML through p38alpha-mediated feedback activation of mTOR signaling, Oncotarget 7 (2016) 37407–37419.
[61] T. Rzymski, M. Milani, D.C. Singleton, A.L. Harris, Role of ATF4 in regulation of autophagy and resistance to drugs and hypoxia, Cell Cycle 8 (2009) 3838–3847.
[62] R. Willows, M.J. Sanders, B. Xiao, B.R. Patel, S.R. Martin, J. Read, J.R. Wilson, J. Hubbard, S.J. Gamblin, D. Carling, Phosphorylation of AMPK by upstream kinases is required for activity in mammalian cells, The Biochemical Journal 474 (2017) 3059–3073.
[63] M.G. Signorello, G. Leoncini, Activation of CaMKKbeta/AMPKalpha pathway by 2-AG in human platelets, J. Cell. Biochem. 119 (2018) 876–884.
[64] N.D. Roe, J. Ren, Oxidative activation of Ca(2+)/calmodulin-activated kinase II mediates ER stress-induced cardiac dysfunction and apoptosis, Am. J. Physiol. Heart Circ. Physiol. 304 (2013) H828–H839.
[65] H.J. Kwon, Y.S. Won, O. Park, B. Chang, M.J. Duryee, G.E. Thiele, A. Matsumoto, S. Singh, M.A. Abdelmegeed, B.J. Song, T. Kawamoto, V. Vasiliou, G.M. Thiele, B. Gao, Aldehyde dehydrogenase 2 deficiency ameliorates alcoholic fatty liver but worsens liver inflammation and fibrosis in mice, Hepatology 60 (2014) 146–157.
[66] H.J. Wang, P.F. Kang, W.J. Wu, Y. Tang, Q.Q. Pan, H.W. Ye, B. Tang, Z.H. Li, Q. Gao, Changes in cardiac mitochondrial aldehyde dehydrogenase 2 activity in relation to oxidative stress and inflammatory injury in diabetic rats, Mol. Med. Rep. 8 (2013) 686–690.
[67] P. Kong, P. Christia, N.G. Frangogiannis, The pathogenesis of cardiac fibrosis, Cell. Mol. Life Sci. 71 (2014) 549–574.
[68] D.L. Maass, J. White, J.W. Horton, IL-1beta and IL-6 act synergistically with TNF-alpha to alter cardiac contractile function after burn trauma, Shock 18 (2002) 360–366.
[69] Y. Zhang, S.L. Mi, N. Hu, T.A. Doser, A. Sun, J. Ge, J. Ren, Mitochondrial aldehyde dehydrogenase 2 accentuates aging-induced cardiac remodeling and contractile dysfunction: role of AMPK, Sirt1, and mitochondrial function, Free Radic. Biol. Med. 71 (2014) 208–220.